Edited Book

Progressive Techniques In Science & Technology Vol -I

Innovative Scientific Publication

Editors

Dr. Nitin K.Mandavgade | Ms. Aachal Lonhare

Nikita Nigam | Dr. Jayant D. Supe

Edited E- Book

On

Progressive Techniques in Science & Technology Vol -I

Editors

Dr. Nitin K. Mandavgade

Professor, Mech Dept, VIT, Nagpur

Ms. Aachal Lonhare

Assist. Prof. Biotechnology, GD Rungta College of Science & Technology ,Bhilai

Nikita Nigam

Assist. Prof. Biotechnology, GD Rungta College of Science & Technology ,Bhilai

Dr.Jayant D.Supe

Associate Professor, Civil Dept, Rungta College of Engineering ,Bhilai

Published by

Innovative Scientific Publication, Nagpur

Published By

Innovative Scientific Publication

SBI Colony, Hingna Road, Nagpur (MS), India

Email: ijiesjournal@gmail.com

Ph: 7972481655

http://ijies.net/books

1st Edition: December, 2023

ISBN: 978-81-965128-9-7

Price: 275 INR

Preface

Science and technology are important parts of our day to day life. We get up in the morning from the ringing of our alarm clocks and go to bed at night after switching our lights off. All these luxuries that we are able to afford are a resultant of science and technology. Most importantly, how we can do all this in a short time are because of the advancement of science and technology only. It is hard to imagine our life now without science and technology. Indeed our existence itself depends on it now. Every day new technologies are coming up which are making human life easier and more comfortable. Thus, we live in an era of science and technology.

Essentially, Science and Technology have introduced us to the establishment of modern civilization. This development contributes greatly to almost every aspect of our daily life. Hence, people get the chance to enjoy these results, which make our lives more relaxed and pleasurable.

We must admit that science and technology have led human civilization to achieve perfection in living. However, we must utilize everything in wise perspectives and to limited extents. Misuse of science and technology can produce harmful consequences.

As we stand on the threshold of a new era, this book aims to explore the transformative "***Progressive Techniques in Science & Technology Vol-I*** " in this book, we delve in to the multifaceted effects to technology on various educational domains, from traditional classroom setting to distance learning environments, we aims to provide educators, policymakers, students and stakeholders with a comprehensive understanding of how technology has reshaped and continues to shape the educational landscape.

We hope that this book serves as a guiding light, inspiring educators and learners alike to embrace innovation responsibly and cultivate an educational environment that nurtures curiosity, critical thinking and lifelong learning.

Dr. N.K.Mandavgade
Ms. Aachal Lonhare
Nikita Nigam
Dr. J.D.Supe

Chapter 1

Exploring the Interplay: The Impact of Anxiety on Decision-Making Processes

***Saroj Nayyar[1], Naveen[2], Bindu Kashyap[3]**

[1]Assistant Professor, Dept of Education, Kalinga University, Raipur
[2]Research Scholar, Amity University, Haryana
[3]Assistant Professor, Dept of Computer Science, GD Rungta College of Science & Technology, Bhilai

ABSTRACT-

This research explores the intricate interplay between anxiety and decision-making processes among college students. Drawing from findings published in the Asian Journal of Psychiatry, the study reveals that a significant percentage of Indian university students experience varying degrees of anxiety, with 37.7%, 13.1%, and 2.4% facing moderate, severe, and extremely severe anxiety, respectively. These figures align with global trends, highlighting elevated anxiety levels among university students worldwide and emphasizing the severity of the issue through alarming suicide rates. The research aims to assess the influence of anxiety on decision-making styles, examining rational, intuitive, dependent, avoidant, and spontaneous styles. A comprehensive review of related studies underscores the need for a deeper understanding of the relationship between anxiety and decision-making. The study adopts a descriptive survey methodology, involving 440 final-year college students selected through simple random sampling. Data collection involves the use of an Anxiety Scale developed by Dr. Kranti K Srivastava and a General Decision-Making Scale adapted from Scott & Bruce. Statistical analysis, including MANOVA and post hoc tests, is conducted using SPSS 28.0.0 version. The results reject the null hypothesis, indicating a significant contribution of anxiety to decision-making styles, particularly in the avoidant style. Further analysis through ANOVA reveals that anxiety significantly influences the avoidant decision-making style. The mean scores indicate a noteworthy difference between high and low anxiety groups, with low anxiety associated with higher avoidant quality. However, no significant effects of anxiety are found on rational, intuitive, dependent, and spontaneous decision-making styles. The study's findings have important educational implications, suggesting the need for targeted interventions and support systems to address and mitigate the impact of anxiety, especially in relation to the avoidant decision-making style. Understanding these nuances can contribute to the development of tailored strategies aimed at fostering positive decision-making outcomes in educational settings.

KEYWORDS: Anxiety, Decision Making, Rational, Intuitive, Dependent, Spontaneous.

INTRODUCTION-

According to findings published in the Asian Journal of Psychiatry, a significant percentage of students in Indian universities experience various levels of Anxiety. Studies indicate that 37.7%, 13.1%, and 2.4% of students are grappling with moderate, severe, and extremely severe Anxiety, respectively. This prevalence aligns with global trends, as study conducted by **Chen et al. (2013)** have highlighted elevated levels of Anxiety and stress among university students worldwide. The severity of the issue is further underscored by alarming suicide rates, with statistics revealing that 6.77 students across different age groups take their own lives in India on a daily basis. Given these concerning figures, it is imperative to establish supportive measures to help students cope with the challenges they face. Individuals afflicted with anxiety disorders often find their capacity to adapt and function proficiently in routine activities, such as work and social engagements, hindered by elevated anxiety levels. Although it is clear that pathological anxiety significantly impacts the daily decision-making of these individuals, a more profound comprehension of the intricate interplay between anxiety

and decision-making is essential. The association between anxiety and deviations in behavior, particularly in response to potential negative outcomes, has long been recognized. Decision-making is a structured procedure that encompasses recognizing and comprehending a problem or issue, acquiring information from various sources, pinpointing alternative solutions, assessing the advantages and disadvantages of each option, choosing the most optimal course of action, implementing the decision, and subsequently assessing both the decision and its outcomes. Rational, intuitive, Dependent, Avoidant and Spontaneous these are the various styles of decision making which used by the students as well as any person who struggles or faces problems in their life in variety of difficult circumstances. Additionally, it serves as a type of problem-solving, where an individual's decisions contribute to resolving a particular issue. This process involves ongoing engagement with the environment to attain desired objectives.

REVIEW OF RELATED STUDIES-

Balugade (2021) not found any differences between female sport students from rural and urban areas in terms of hostility or anxiousness. **Choudhury & Shejith (2021)** explored a distinct relationship between behavioural young adults with social anxiety. **D'Souza & Srivastava (2021)** decleared that people with poor self-efficacy experienced a decline in their academic performance mean scores. **Nayak & Bhatt (2021)** not found any discernible difference between males and girls in terms of emotional quotient, but a discernible difference experienced between them in terms of anxiety. **Wadhawan et al. (2021)** explored that young boys and girls will not differ in terms of their level of anxiety. **Jang (2022)** investigated that self-confidence and dependent type were significantly associated with anxiety with clinical decision making. **Jiang et. al. (2022)** found educational and family stress significantly leads to Anxiety among students, negatively affecting their academic performance and learning outcomes. **Ran et. al. (2022)** declared a significant relationship between EI, GSE, and career decision-making difficulties. Results revealed a significant positive relationship of GSE with emotional intelligence. GSE has a significant negative relationship with career decision-making difficulties.

OBJECTIVE-

To assess the influence of Anxiety on Decision Making Styles.

HYPOTHESIS-

H_0- There will be no noteworthy contribution of Anxiety on Decision Making Styles**.**

METHODOLOGY-

- **Sample & Sampling techniques-** 440 students of college going have been taken through simple random sampling technique.
- **Research Design-** Independent Variable- Anxiety
  Dependent Variable- Decision Making styles- Rational, Intuitive, Dependent, Avoidant, Spontaneous.
- **Tool used-** Anxiety Scale developed by Dr. Kranti K Srivastava (2021) which is two point Likert scale having 30 items and General Decision-Making Scale Indian adapted version of Scott & Bruce (1995) having 25 items used to collect data.
- **Research Type-** Descriptive survey method.
- **Data Analysis-** Following data collection, the data were coded, imported into SPSS 28.0.0 version for statistical analysis, and MANOVA has been employed.

ANALYSIS AND RESULT-

H_0 There will be no noteworthy contribution of Anxiety on Decision Making styles
To examine the independent variable Anxiety, MANOVA has been used to test the main effect on various decision making styles.

Table-1

MANOVA summary for Anxiety on scores of various styles of Decision Making

Effect	Value	F	Hypothesis df	Error df	p value	Partial Eta Squared	Effect
Anxiety	Pillai's Trace	.040	3.627**	5.000	436.000	.003	.040
	Wilks' Lambda	.960	3.627**	5.000	436.000	.003	.040
	Hotelling's Trace	.042	3.627**	5.000	436.000	.003	.040
	Roy's Largest Root	.042	3.627**	5.000	436.000	.003	.040

From the above table 1 main effect of anxiety is showing statistically significant Wilks' Lambda =.960, F(5,436=3.627), values for Pillai's Trace test (.040, F(5,436=3.627)), Hotelling's Trace and Roy's Largest Root (.042, F(5,436=3.627)) All these values found to be significant.

Hence the null hypothesis "There will be no noteworthy contribution of Anxiety on Decision Making styles" is **rejected**. One way MANOVA cannot tell which specific groups are significantly different from another. For further analysis researcher has been conducted post hoc test.

Post Hoc Test

To determine the contribution of anxiety on various decision making styles analysis of variance or ANOVA was conducted and level of significance is .05 and .01 has been settled by the researchers.

Table-2

ANOVA table for various styles of Decision Making

Source		Sum of Squares	df	Mean Square	F (ANOVA)
Anxiety	Rational	.856	1	.856	0.025
	Intuitive	8.819	1	8.819	0.675
	Dependent	4.394	1	4.394	0.254
	Avoidant	370.429	1	370.429	17.468**
	Spontaneous	3.091	1	3.091	0.214
Error	Rational	15348.735	440	34.883	
	Intuitive	5752.197	440	13.073	
	Dependent	7621.016	440	17.320	
	Avoidant	9330.944	440	21.207	
	Spontaneous	6340.911	440	14.411	

- **Main effect of Anxiety on Rational first Decision making style**

In table 2 the main effect of Anxiety on **Rational** was not found to be significant [(1/440) =0.025, p > .05] which is less than standard value 3.84, therefore Anxiety does not influences the Rational the first Decision making style.

- **Main effect of Anxiety on Intuitive second Decision making style**

In table 2 the main effect of Anxiety on **Intuitive** was not found to be significant [(1/440) =0.675, p > .05] which is less than standard value 3.84, therefore Anxiety does not influences the **Intuitive** second Decision making

style.

- **Main effect of Anxiety on Dependent third Decision making style**

In table 2 the main effect of Anxiety on **Dependent** was not found to be significant [(1/440) =0.254, p > .05] which is less than standard value 3.84, therefore Anxiety does not influences the **Dependent** third Decision making style.

- **Main effect of Anxiety on avoidant forth style of Decision making**

In table 2 the main effect of **Anxiety** on **avoidant** was found to be significant [(1/440) = 17.468, p < .01] which is greater than standard value 6.90, therefore **Anxiety** influences the **avoidant** forth Decision making style.

Table-6

Showing the main effect of Anxiety on avoidant forth decision making style

Anxiety	N	Mean	Standard Deviation
High	159	13.28	3.09
Low	281	18.11	3.87

It was observed from Table 5 that mean value of **avoidant** with high anxiety is 13.28 whereas mean value of **avoidant** with low anxiety is 18.11 so it can be concluded that low anxiety produces the high **avoidant** quality.

Graphical Representation Of Mean And Standard Deviation Scores Of Avoidant In Relation To Anxiety

Figure-1

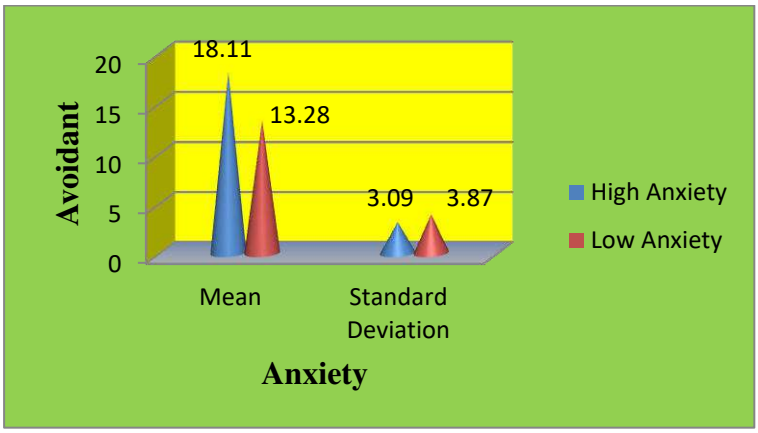

- **Main effect of Anxiety on spontaneous fifth Decision making style**

In table 2 the main effect of **Anxiety** on **spontaneous** was not found to be significant [(1/440) =0.214, p > .05] which is less than standard value 3.84, therefore **Anxiety does not** produces the main effect on **spontaneous** fifth Decision making style.

DISCUSSION-

Main influences of Anxiety on Rational, Intuitive, Dependent and Spontaneous has been not found whereas Main impact of Anxiety on Avoidant has been clearly seen with noteworthy difference.

SUGGESTIONS AND EDUCATIONAL IMPLICATIONS-

In showcasing competence, enthusiasm, and accomplishments in life, students need to possess the capacity for decision-making. Those with robust mental well-being and effective decision-making capabilities have the potential to forge promising paths ahead. Furthermore, students maintaining stable mental health can successfully navigate challenges across diverse domains, leading to favorable academic performance. Educational institutions should take initiatives aligned with students' decision-making process to enhance their overall development. **Educational Significance of Findings**: The study reveals that anxiety does not exhibit significant influences on rational, intuitive, dependent, and spontaneous decision-making styles. However, a distinct impact is observed in the case of the avoidant decision-making style, indicating a substantial and noteworthy difference. These findings have important implications for educational practices, suggesting a need for targeted interventions and support systems to address and mitigate the impact of anxiety, particularly in relation to the avoidant decision-making style. Understanding these nuances can contribute to the development of tailored strategies aimed at fostering positive decision-making outcomes in educational settings.

REFERENCES-

[1] *Balugade, A. B. (2021). A Study of Anxiety and Aggression Between Rural and Urban Female Sport Students. International Journal of Indian Psychology, 9(2), 1049-1053. DIP:18.01.109.20210902, DOI:10.25215/0902.109.*

[2] *Chen, L., Wang, L., Qiu, X. H., Yang, X. X., Qiao, Z. X., Yang, Y. J., & Liang, Y. (2013). Depression among Chinese university students: Prevalence and socio-demographic correlates. PLoS ONE, 8(3), Article e58379. https://doi.org/10.1371/journal.pone.0058379*

[3] *D'Souza, I. & Srivastava, A. (2021). Effect of Self-efficacy, Motivation and Anxiety on Online Academic Performance. International Journal of Indian Psychology, 9(2), 1932-1959. DIP:18.01.192.20210902, DOI:10.25215/0902.192*

[4] *Jang, Eun-Hee. (2022). The Influence of metacognition, decision-making type on self-confidence and anxiety with clinical decision making of nursing students. Korean Association for Learner-Cantered Curriculum and Instruction. 22. 253-265. https://www.researchgate.net/publication/366406293_The_Influence_of_metacognition_decision-making_type_on_self-confidence_and_anxiety_with_clinical_decision_making_of_nursing_students/citation/download*

[5] *Jiang, Z., Jia, X., Tao, R., & Dorduncu, H. (2022). COVID-19: A Source of Stress and Depression Among University Students and Poor Academic Performance. Frontiers in public health, 10, 898556. https://doi.org/10.3389/fpubh.2022.898556*

[6] *Nayak, S. & RKrishnan, B. (2021). Emotional Intelligence and Anxiety among Under Graduate Students. International Journal of Indian Psychology, 9(2), 781-788. DIP:18.01.083.20210902, DOI:10.25215/0902.083*

[7] *Ran, Z. O. U., Zeb, S., Nisar, F., Yasmin, F., Poulova, P., & Haider, S. A. (2022). The impact of emotional intelligence on career decision-making difficulties and generalized self-efficacy among university students in China. Psychology Research and Behavior Management, 865-874. https://www.tandfonline.com/doi/full/10.2147/PRBM.S358742*

[8] *RoyChoudhury, N. & Shejith R. (2021). A Study on Social Anxiety and Aggression among Young Adults. International Journal of Indian Psychology, 9(4), 179-184. DIP:18.01.019.20210904, DOI:10.25215/0904.019*

[9] *Wadhawan, P., Sran, S. & Vats, P. (2021). Gender Differences in the Level of Anxiety of Young Adults During COVID-19. International Journal of Indian Psychology, 9(2), 654-662. DIP:18.01.069.20210902, DOI:10.25215.0902.069*

Chapter 2

Tissue Culture and Spawn Preparation of Edible Mushroom (*Agaricus Bisporus*)

***Siddhant Khare[1], Ujjwala Supe[2], Doly John[3]**

[1]Department of Chemistry, Sai College, Bhilai
[2,3]Department of Biotechnology, St. Thomas College, Bhilai

ABSTRACT

Among the Higher Basidiomycota, the white button mushroom (*Agaricus bisporus*) is a crucial food and medicinal species that is utilized in the recycling of agricultural waste. includes debris from reed plants, wheat straw, and rubbish Paper, discarded tea leaves, oat straw, a few water plants, and others. There are several uses for *Agaricus bisporus* in human diets and due to its mix of key components, pharmaceutical carbs, fatty acids, amino acids, and low calorie vitamins, trace minerals, and unprocessed fibers. This paper demonstrates the process of tissue culture and spawns preparation for the cultivation of white button mushroom (*Agaricus bisporus*) Potato dextrose agar is used as the culturing media. The mushroom culture can be prepared in both slant and Petri plates. Various methods should be followed for the production of spawn and the standardized spawn will be prepared after the growth of mycelium in pure culture and subculture with the help of wheat mixed with calcium carbonate and calcium sulfate. Two types of spawning techniques have been used alternate spawning method and the top layer spawning method. As a result, the alternating spawning method gives good results in the harvesting fruit body of mushrooms.

INTRODUCTION

Agaricus bisporus, is the most familiar mushroom for most of us. it is the commercial mushroom sold in stores and put on pizza. It comes in various forms: button versions, brown versions and large portobello versions all of which are varieties of the same species. Its popularity is not so much a consequence of flavor as it is a consequence of its suitability for commercial production. *Agaricus* does grow wild, typically in fields or lawns but all of the *Agaricus* mushrooms sold in stores are grown on a controlled medium and in a controlled Environment. (Barros et al., 2008). Mushrooms have a unique texture have good aroma, taste and flavor that differs mushroom from other food crops. Edible species of mushrooms found abundantly in indigenous forests. Mushrooms are highly nutritive, low-calorie food with good quality proteins, vitamins and minerals. Mushrooms are an important natural source of foods and medicines. By virtue of having high fiber, low fat and low starch, edible mushrooms have been considered to be ideal food for obese persons and for diabetics to prevent hyperglycaemia. They are also known to possess promising anti oxidative, cardiovascular, hypercholesterolemia, antimicrobial, hepato-protective and anticancer effects. Fekadu Alemu (2014)

MATERIALS AND METHODS

Preparation of bacteriological media:

Potato Dextrose Agar
Readymade Potato Dextrose Agar base media (Hi Media) was used. Agar powder was added to basal media.

Collection of Mushroom samples

One species of mushrooms, *Agaricus bisporus* (were collected from local markets placed in sterile Polyethylene bags and kept at a temperature of 4 ºC until use). The material was brought to the laboratory and preserved at room temperature.

PREPARATION OF MOTHER CULTURE OF MUSHROOM

Mother culture production: Fruiting bodies of white fungi *Agaricus bisporus* strain were used for producing pure mother culture by the method of tissue culture in Petri dishes contained the Potato Dextrose Agar (PDA) media. Then, the dishes were transferred to an incubator with a degree of 25±1^{0}C for three weeks with continuous monitoring for mycelium growth and the exclusion of contaminated dishes. Optimal conditions determination to produce the mother culture: The fungi isolated, purified from the previous step, was developed on two types of media, which is the commercial media Potato Dextrose Agar, which was used to stimulate and preserve the isolates and for comparison.

Effect of the media type on the growth rate of fungi:

The media were mixed well, and its pH was set to 6.5, sterilized in the autoclave device at 121°C for 15 minutes, and it cooled to 55°C, then it was distributed in Petri dishes with a diameter of 8.5 cm. The prepared dishes are inoculated with a piece of stimulated fungi growth on the PDA media, by placing that piece in the center of the dish, and then the dishes were tightly closed with Parafilm. The dishes were incubated at a temperature of 25°C, and the growth of mycelium was monitored until it was fully grown in the dish

Preparation of subculture

Mycelial agar cultures (8 mm diameter) were, taken from the margin of seven days old fungal colonies were inoculated individually in the centre of plates containing PDA medium. The plates were incubated at 28 ± 2°C for seven days.

Preparation of subculture in slants

Mycelial agar cultures (8 mm diameter) were, taken from the margin of seven days old fungal colonies were inoculated individually in the centre of slants containing PDA medium. The slants were incubated at 28 ± 2°C for seven days.

PREPARATION OF SPAWN

Substrate preparation

Good quality wheat grains which were free from pest and moulds were seected. boiled grains were submerged in clean water for 20 – 30 minutes. When the grains become soft, remove and spread evenly on a cotton cloth to drain out the water and cool the grains. We added 20g of $CaCO_3$ and 20 gm of $CaSO_4$ to the grain mixed well. Fill 250 gms of grain in cleaned and dried polypropylene bags and plug the mouth of the bottle tightly with non-absorbent cotton. Sterilized the grain bags in autoclave exposed to 121^{0}c for 20 minutes. After cooling transfer the bags to inoculation chamber.

Inoculation of substrate

The grain bags on platform were allowed to dry for 1 hr after that, placed the bags in laminar air flow for 20 to 30 min for UV exposure. Inoculation was done by using prepared mother culture .Mycelial agar cultures were placed in bags using inoculation loop. Bag was mixed well and lightly closed with cotton plugs .

Production of spawn

The inoculated bags were shifted to spawn room having temperature range of 25 – 30 ^{0}C. Check the bags regularly and discard contaminated one immediately. Within 15 – 20 days of inoculation mycelial growth covers entire substrate and the spawn is ready for use.

RESULTS AND DISCUSSION

Chapter 2

MOTHER CULTURE

Inoculated mushroom tissue were fully grown in PDA plates in 7days forming the mother culture.

Figure 1 A) the growth of mushroom in subculture plates B) the summary of spawn production C) Growth of mushroom subculture D) Prepared spawn

Spawn preparation

After 2-3 weeks the mushroom mycelium fully colonizes (covers) the wheat grains. To begin with, spawn is prepared in bags using the culture grown in the test tube and this is called Mother Spawn. The first generation grain spawn prepared is Mother Spawn.

Using potato dextrose agar is for developing mushroom culture. The contaminated plates were discarded. And the spawn bags and the mushroom beds which are contaminated and damaged during the growing period and sterilization were discarded. Using the completely cover mycelium covered spawn the bags were prepared and the spawns and the beds were s during the incubation period. The contaminants were discarded to avoid the spoilage to the nearer bags. mushroom shed were maintained at correct temperature. The mycelium covered within 15 – 25 days in mushroom beds.

CONCLUSION

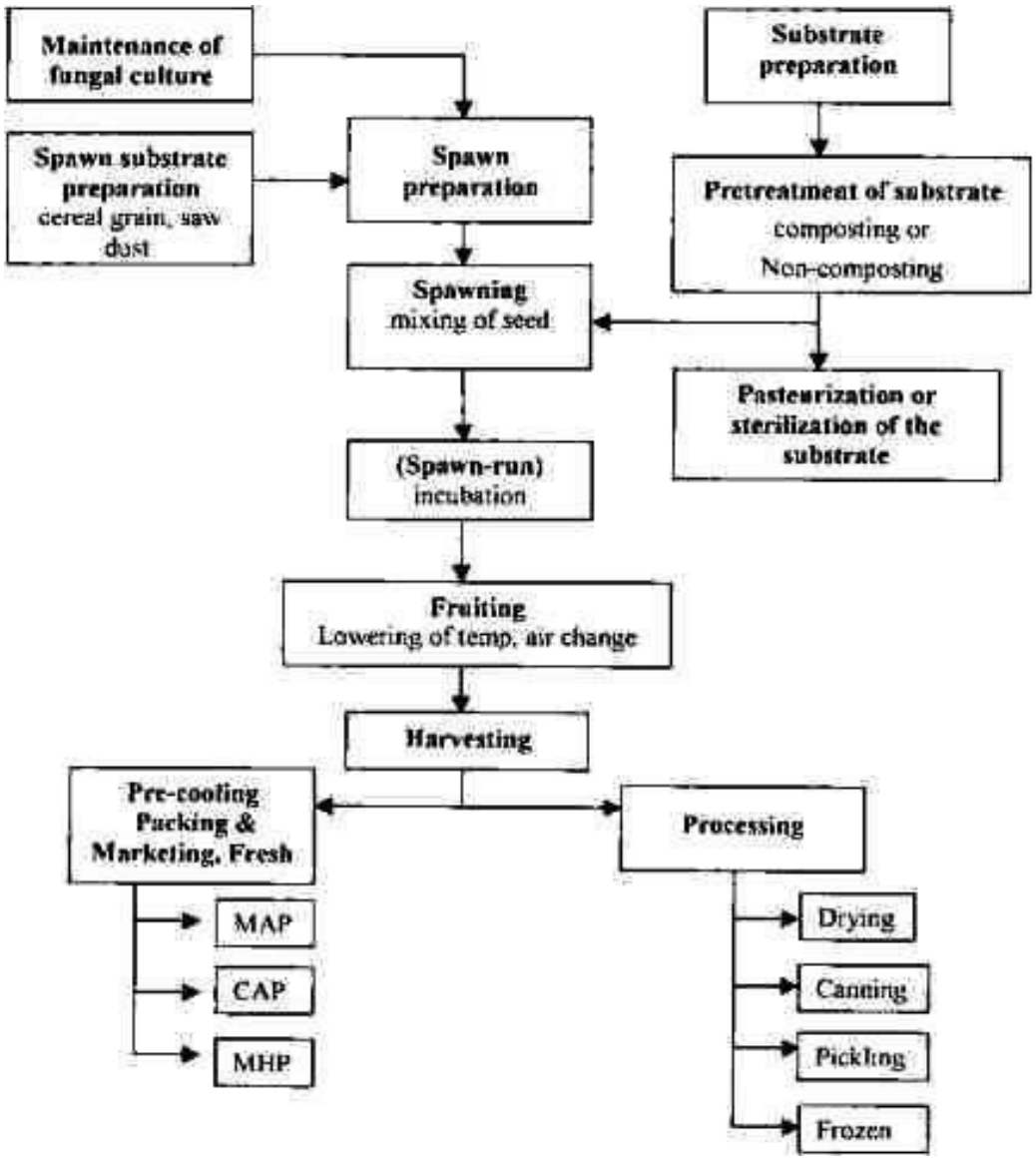

REFERENCES

[1] *Bahukhandi d,and Munjal, R.L.Cultivation of Pleurotus Species on different Agricultural Residues. India Phytopath. 42(4), 1989.492-495.*

[2] *Barros L, Cruz T, Baptista P, Estevinho LM, Ferreira IC (2008) Wild and commercial mushrooms as source of nutrients and nutraceuticals. Food Chem. Toxicol 46(8): 2742-2747.*

[3] *Fekadu Alemu (2014) Cultivation of lentinus edodes on teff straw (agricultural residue) at Dilla University, Ethiopia, Applied Microbiology 1(3): 49-59.*

[4] *Fekadu Alemu (2014) Cultivation of pleurotus ostreatus on grevillea robusta leaves at Dilla University, Ethiopia, Journal of yeast and Fungal Research 5(6): 74-83.*

[5] *Fekadu Alemu (2015) Cultivation of Shiitake Mushroom (Lentinus edodes) on Coffee Husk at Dilla University, Ethiopia, Journal of Food and Nutrition Sciences 3(2): 63-70.*

[6] *Manjunathan J, Kaviyarasan V (2010) Nutrient composition in wild and cultivated edible mushroom, Lentinus tuberregium (Fr.) Tamil Nadu, India. International Food Resource. Journal 18(2): 59-61.*

[7] *Hrudayanath T, Sameer KS (2014) Diversity, nutritional composition and medicinal potential of Indian mushrooms, African journal of Biotechnology, Biju Patnaik University of Technology, Bhubaneswar, Odisha, India.*

Chapter 3

Performance Analysis of Smoke Tube Boiler for Waste Heat Recovery

Shaikh Alam[1], Shriram M. Ughade[2*]

[1]Department of Mechanical Engineering, RKNEC Nagpur (MH), India
[2]Department of Mechanical Engineering, SCET Nagpur (MH), India

ABSTRACT

Waste heat recovery is the recovery of waste heat from hot fluids that can be reused again for other processes. Waste heat recovery can be done through various waste heat recovery technologies to provide valuable energy sources and reduce the overall energy consumption. In the present work, performance analysis of smoke tube boiler for waste heat recovery is carried out. The main objectives of this work are to analyze the existing waste heat recovery system for smoke tube boiler and carryout simulation of existing waste heat& improvement in waste heat recovery system for smoke tube boiler. For validation, analytical results are compared with simulation results.

Keywords: Waste heat recovery, Boiler, heat exchanger, mixing chamber, mass transfer

1. Introduction

Industrial waste heat refers to energy that is generated in industrial processes without being put to practical use. Sources of waste heat include hot combustion gases discharged to the atmosphere, heated products exiting industrial processes, and heat transfer from hot equipment surfaces. Waste heat recovery entails capturing and reusing the waste heat in industrial processes for heating or for generating mechanical or electrical work. Example uses for waste heat include generating electricity, preheating combustion air, preheating furnace loads, absorption cooling, and space heating. Heat recovery technologies frequently reduce the operating costs for facilities by increasing their energy productivity. Many recovery technologies are already well developed and technically proven; however, there are numerous applications where heat is not recovered due to a combination of market and technical barriers [14].

In the present work, performance analysis of smoke tube boiler for waste heat recovery is carried out at JSW Steel Coated Products Limited Kalmeshwar, Nagpur (MH). In the existing waste heat recovery smoke tube boiler, volatile organic compound from prime oven and finish oven of color coating line is sucked by exhaust blower and passes through Regerative Thermal Oxidizer (RTO) where volatile organic compound gets decomposes into flue gas. The flue gas is passed in mixing chamber where the temperature of flue gases reduces by mixing of proper amount of fresh air supplied by blower in mixing chamber. The flue gases is then passed in heat exchanger where flue gases and fresh air is heated. The temperature of outlet fresh air after heat exchanger is maintained by controlling the bypass valve which control the air flow to chimney. The heat recovered from heat exchanger is then send to the prime and finish oven of color coating line for preheating process. The heat exchanger then supplies the flue gases to boiler where temperature of gases gets reduced and this gases is passed in atmosphere through chimney.

Chapter 3

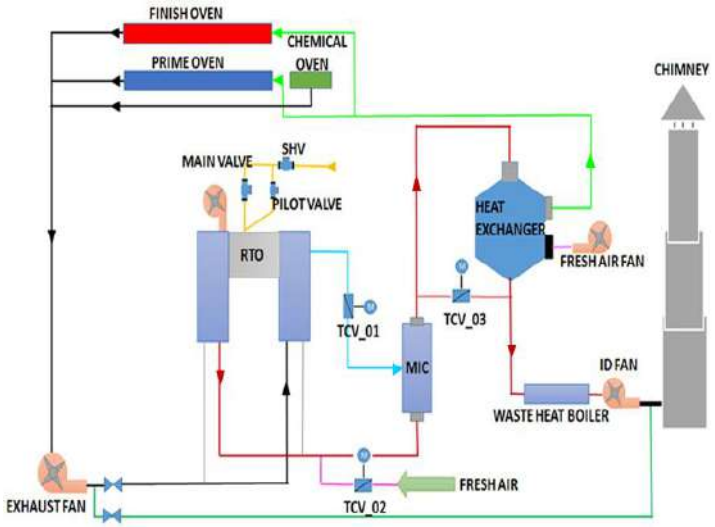

Fig.1. Existing waste heat recovery smoke tube boiler system

Nomenclature

Q	Heat transfer rate (w)
L	Tube length (m)
t	Tube thickness (m)
Nt	No. of Tubes (units)
Cp	Specific Heat Capacity (kJ/kgK)
Thi	Hot fluid inlet Temperature (K)
Tci	Cold fluid inlet Temperature (K)
Tho	Hot fluid outlet Temperature (K)
Tco	Cold fluid outlet Temperature (K)
Uo	Overall heat transfer coefficient (W/m^2k)
Di	Tube inside diameter (m)
Do	Tube outside diameter (m)
De	Equivalent diameter (m)
Ds	Diameter of shell (m)
Nu	Nusselt number
Pr	Prandtl number
Re	Reynolds number
Gs	mass flux (kg/m^2s)
μ	kinematic viscosity (m^2/s)
ρ	Density (kg/m^3)
Kmt	Thermal conductivity of tube material (W/mK)
hi	Shell side heat transfer coefficient (W/m^2k)
ho	Tube side heat transfer coefficient (W/m^2k)
∆Ps	Shell side pressure drop (N/m^2)
∆Pt	Tube side pressure drop (N/m^2)
∆Tm	log mean temperature difference(℃)

Abbreviations

CTP	tube count calculations constant
CL	tube layout constant
STHE	Shell and tube heat exchanger

LMTD	Logarithmic mean temperature difference
PR	Pitch ratio
PT	Tube pitch
t	tube side flow

Subscript

c	cold fluid
h	hot fluid
i	inlet conditions
o	outlet conditions
s	shell side flow

2. LITERATURE REVIEW

Panagiotis Drosatos et al. proposed an in-house built code and its incorporation into an ANSYS FLUNT Computational Fluid Dynamics (CFD) model for the simulation of the convection section of a boiler.

A. Zargoushi et al. Developed a CFD model in ANSYS FLUENT to understand transport phenomena, especially the phase change in a complex plate-fin heat exchanger operated in a gas refining company. Three models local thermal equilibrium between the porous medium and fluid flow without mass transfer(LTE-non mass), local thermal equilibrium between the porous medium and fluid flow with mass transfer(LTE), and local thermal non- equilibrium between the porous medium and fluid flow with mass transfer(LTNE) have been evaluated in this paper. Among three model, LTNE with mass transfer provides better results than those of LTE and LTE without mass transfer.

Chamil Abeykoon et al. designed and carried out CFD simulation of compact heat exchanger. In this work, six CFD models were developed. On the basis of CFD results, it was found out that a selection of parameters such as a the baffle cut ratio, number of baffles , tubes flow and tube arrangements are important in optimizing the performance of a shell and tube heat exchanger.

Wei-Wei Wang et al. carried out the mathematical and CFD numerical investigation of a radial heat pipe.CFD results indicates that present built volume of fluid model can effectively reproduce phase change fluid flow and heat transfer inside radial heat pipe. Numerical modeling results were validated by the experimental tests for various conditions and maximum deviation fall within 10%.

M.A. Gomez et al. studied about the influence of exhaust gas recirculation and oxygen excess ratio in a biomass fed with pure oxygen. A theoretical model for simulation of biomass combustion is proposed through additional in built routines on a CFD commercial code. The model implements several sub models of thermal conversion of solid biomass as well as heat and mass transfer, chemical reactions and radiation transport to solve the behavior of a boiler in a steady situation with a relatively low computational cost.

Ram Thakar et al. Recovered waste heat energy of exhaust gas of diesel engine by placing specially designed heat exchanger near the inlet and outlet duct of the engine in order to used exhaust energy for preheating the air passed to the engine. The heating of inlet air improves the performance of the diesel engine and reduces the emission level. The effectiveness of heat exchanger found to be 0.615.

Elloit Woolley et al. studied how an industrial waste heat recovery is done. They studied about availability of waste heat energy, the ability to recover and to reduce industrial energy costs and environmental impacts. They developed a waste heat energy recovery framework to provide manufacturers with a four step methodology in assessing production activities in facilities, analyzing the compatibility of waste heat source sink in term of energy balance and temporal availability, selecting appropriate heat recovery technologies and decision support based on economic benefits.

M.C. Barma et al. studied about amount of energy used in boiler, various losses and causes occurred in boilers and how to minimized heat loss using various technologies. Energy saving measures in boiler is also discussed in this study. Different types of energy saving techniques such as excess air control, improving combustion efficiency, utilization of waste heat content of flue gases etc., have been reviewed in this study.

Ratchaphon Suntivarakorn et al. carried out the experiment to improve the efficiency of a fire tube boiler with a fixed gate and screw conveyor for feeding fuel. The experiment result shows that using heat recovery and fuel drying reduces 3% weight of fuel moisture content and boiler efficiency increases 0.41%.

Shubham Agarwal et al. studied about boiler maintenance and various possible causes responsible for the breakdown of the boiler. Different research approaches have been discussed related to the material of the boiler and its components, regarding various hazards possible in the boilers. A maintenance schedule has also been prepared so as to optimize different maintenance actions.

M. Manickam et al. developed model of waste heat boiler for utilizing plant off-gas consisting of gaseous and particulate combustibles. This model can allows various calculations like temperatures of gas and particles within the boiler. Mixing in the burner region, char burnout and char particles temperature were analyzed using this model. Combustion stability also studied using Eddy break-up model which accounts for combustion kinetics and the results obtained are compared with a mixed-is-burnt model.

3. OBJECTIVES

a) To analyze the existing waste heat recovery system for smoke tube boiler.
b) To carryout simulation of existing waste heat recovery system for smoke tube boiler.
c) To identify the scope of improvement in waste heat recovery system for smoke tube boiler.

4. METHODOLOGY

In the methodology, first the detailed study of smoke tube boiler is carried out. After that performance analysis of existing waste heat recovery boiler is done and analytical design of boiler is prepared. After analytical design, the CFD model in ANSYS FLUENT is developed and CFD results are validated.

5. ANALYTICAL DESIGN

Available data for calculations:-

1. Type of boiler – smoke tube boiler
2. Tube length (L) – 6m
3. Internal diameter of tube (Di) = 44.3mm
4. Outer diameter of tube (Do) = 50.8mm
5. Mass flow rate of flue gases (mh) = 0.53kg/sec
6. Mass flow rate of water=0.183kg/sec
7. Number of tubes in boiler (Nt) = 599
8. Inlet temperature of flue gas (Thi) = 310º C
9. Inlet (Tci) & Outlet temperature (Tco) of water = 30º C & 100º C
10. Specific heat of flue gas (Cph) =1.122kJ/kgK & specific heat of water(Cpc)= 4.183kJ/kgK

Heat available for waste heat recovery system

$Q = (mh \times Cph \times \Delta T)$ flue gases

$= 0.53 * 1.122 * (310-30)$

$= 166.50$ kW

Where,

Q =heat transfer rate (W)
mh= mass flow rate of flue gases (kg/sec.)
Cph = specific heat of flue gases (kJ/kgK)

By applying law of conservation of energy to boiler:-

Heat supplied by gas =Heat absorbed by water
(mh×Cph×ΔT) flue gases = (mc×Cpc×ΔT) water
0.53*1.122*(310-Tho) = 0.183*4.183*(100-30)
Tho = 220^0C

Amount of heat energy required for heating water
Q = 0.183*4.183*(100-30) = 53.58KW

Preliminary Analysis of Shell & Tube Exchanger(Boiler)
Following parameters value taken from TEMA Standard[8]

1. Single shell single pass Heat exchanger (CTP=.93)
2. Tube layout (CL=1)
3. Length of tube (L) =6m
4. Tube inside diameter (Di) =44.3 mm
5. Tube outside diameter (Do) =50.8 mm
6 .Tube material steel (Kmt) = 26.1 W/mK
7. Pitch ratio (PR) =1.25
8. Baffle space=0.6Ds
9. Baffle cut=0.25Ds
10. hi=100 W/m²K ho=4000 W/m²K

A. Overall heat transfer coefficient
a. Without considering the fouling factor (Uo)

$$Uo = \frac{1}{\frac{1}{hi} * \frac{ro}{ri} + \ln\left(\frac{ro}{ri}\right)\left(\frac{ro}{k}\right) + \frac{1}{ho}}$$

= 84.38W/m²K

b. With fouling factor
Rfo=0.0001754m²K/W

$$Uf = \frac{1}{\frac{1}{hi} * \frac{ro}{ri} + \ln\left(\frac{ro}{ri}\right)\left(\frac{ro}{k}\right) + \frac{ro}{ri} * Rf + \frac{1}{ho}}$$

= 69.82W/m²K

B. Properties of fluids

	Flue gas	water
Density (kg/m3)	0.6825	985
Specific heat (kJ/kgK)	1.109	4.183
Thermal conductivity (W/mK)	0.044	0.6513
Kinematic viscosity (m²/s)	$39.30 * 10^{-6}$	$0.478 * 10^{-6}$
Prandtl No.(Pr)	0.66	3.020

C. LMTD for counter flow heat exchanger (Boiler)

$$\Delta Tm = \frac{\Delta T1 - \Delta T2}{\ln\left(\frac{\Delta T1}{\Delta T2}\right)}$$

$= 200^0C$

1. Area of heat exchanger

Q = U*A*ΔTm

Area = 3.79m²

2. Shell side diameter (Ds)

$$Nt = 0.785 * \frac{CTP \quad Ds^2}{CL \quad PR^2 * Do^2}$$

Ds = 1.81m

Where,

CTP = tube count calculations constant (1 tube pass = 0.93)

CL = tube layout constant (CL = 1)

PR = pitch ratio (1.25)

3. Baffles space=0.6*Ds=1.086m

4. Baffle cut=0.25*Ds=0.4525m

5. **Mc Adam equation,**

$$\frac{ho * De}{k} = 0.36 \left(\frac{De * Gs}{\mu}\right)^{0.55} * \left(\frac{Cp * \mu}{k}\right)^{0.33} * \left(\frac{\mu b}{\mu w}\right)^{0.14}$$

Where,

De- equivalent diameter of the shell side

K,μ and Cp- fluid properties on shell side at bulk mean temperature

Gs- shell side mass velocity

μw - viscosity at wall temperature
μb – viscosity at bulk mean temperature

$$De = \frac{4 * (Pt^2 - \frac{\pi}{4} * Do^2)}{\pi * Do}$$

= 0.050m

$$Gs = \frac{m}{As}$$

=0.53/0.03931
= 1.34kg/m²s

D. Shell side pressure drop

$$\Delta Ps = \frac{f * Gs^2 * (Nb + 1)Ds}{2 * \rho * De * \varphi s}$$

$$f = \exp\{0.576 - 0.19\ln(Re)\}$$

f = 0.4326

Where, f = friction factor
Nb = no. of baffles

ΔPs = 114.44N/m²

G. Tube side pressure drop

$$\Delta Pt = \frac{4 * Np * \rho * Uin^2}{2}\left(\frac{f * L}{Di} + 1\right)$$

$$At = \frac{\pi}{4} * Di^2 * \frac{Nt}{Np}$$

At = 0.9232m²

$$Uin = \frac{mt}{\rho * At}$$

Uin = 0.000198 m/s

ΔPt = 0.00460 N/m²

6. COMPUTATIONAL FLUID DYNAMICS (CFD) DESIGN OF HEAT EXCHANGER (BOILER)

Overview of CFD

Computational fluid dynamics (CFD) is a technique of predicting fluid flow, heat transfer, chemical reactions, mass transfer by solving the mathematical equations. The main application of CFD is as an engineering method, to provide data that is complementary to theoretical and experimental data. This is mainly the domain of commercially available codes and in-house codes at large companies. CFD can also be used for purely scientific studies, e.g. into the

fundamentals of turbulence. This is more common in academic institutions and government research laboratories. Codes are usually developed to specifically study a certain problem.

CFD simulation of STHE

CFD simulation of STHE consists of following steps:-

1. Pre-processing
2. Solver set-up
3. Post processing
4. Validation

Geometry creation of model is done in SOLIDWORKS 2016. Geometry of model is created according to the specifications of STHE. After creation of geometry, meshing and discretization of geometry is done. The entire geometry is divided into two fluid domains shell side (flue gas) and tube side (water) in order to have better control over the nodes of elements. After meshing of model, model is imported to FLUENT where simulation is carried out. The model simulated has flue gas as one fluid and water as another fluid. The state of the various portions of the geometry such as fluid or solid is check in the cell zone conditions. Boundary conditions are selected for inlet and outlet of shell and tube.

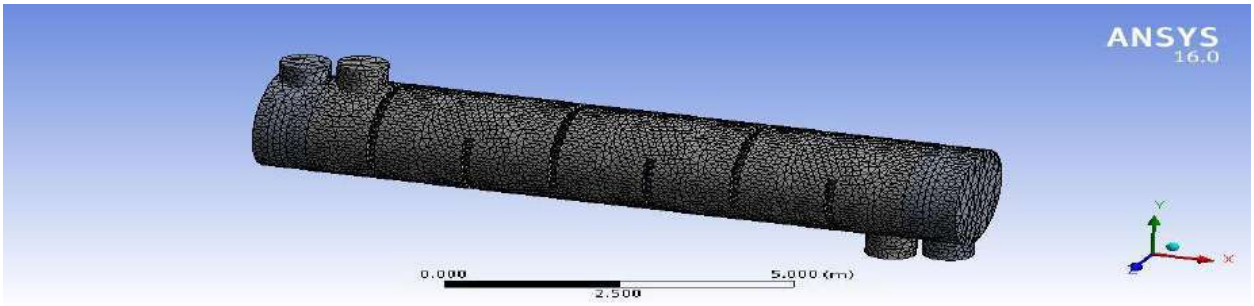

Fig.2.Meshing diagram of shell and tube heat exchanger

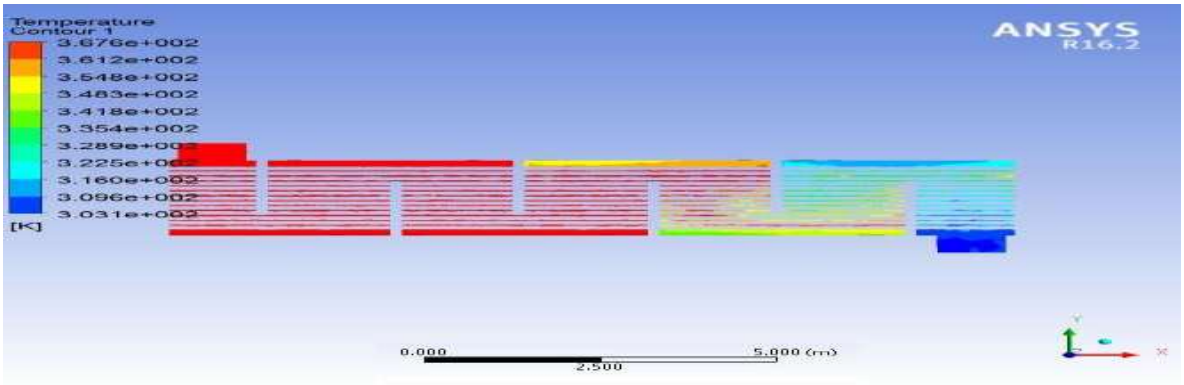

Fig.3.Contours of temperature for water domain(tube side)

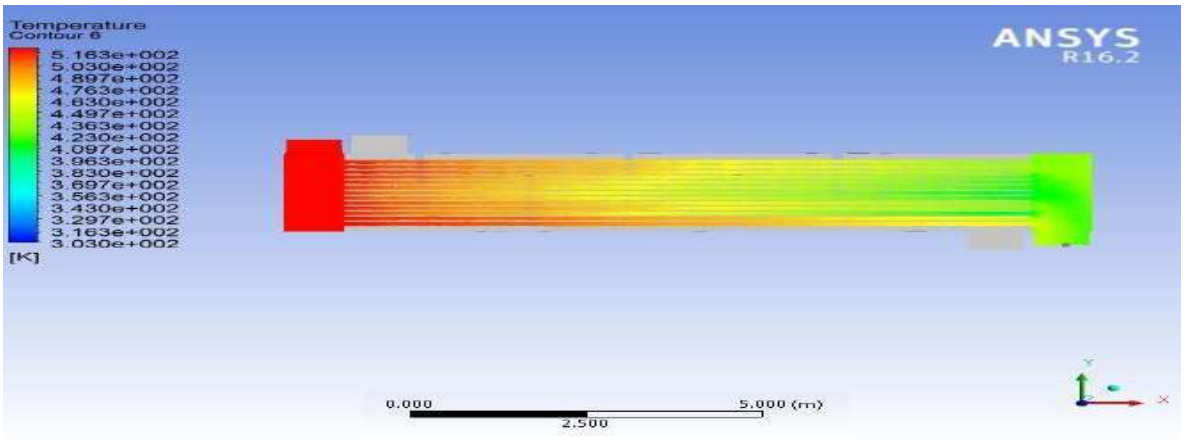

Fig.4.Contours of temperature for flue gas domain(shell side)

CFD simulation results

Fig.3. shows the contours of static temperature for water inside the tube side, in which blue color is the water inlet and orange color is the water outlet. From fig.3. it is seen that the temperature of water increases from 303K to 367K because of heat absorbed by water from the flue gases.

Fig.4. shows the contours of static temperature for flue gas inside the shell side, in which red color portion is the flue gas inlet and blue end is the flue gas outlet. From fig.4. it is seen that the temperature of flue gas drop down from 516K to 303K because of rejection of heat from flue gases to the water.

7. RESULTS AND DISCUSSION

Exit temperature of the flue gases from STHE in analytical analysis was obtained as 220℃, where in CFD simulation it was found to be 242℃. Thus, the percentage error of temperature for the flue gases between analytical calculation and CFD simulation is,

$$\%T_{error} = \frac{T_{analytical} - T_{cfd}}{T_{analytical}}$$

$$=10\%$$

Exit temperature of the water from analytical analysis was obtained as 100℃, where in CFD simulation it was found to be 94.6

$$\%T_{error} = \frac{T_{analytical} - T_{cfd}}{T_{analytical}}$$

$$=5.4\%$$

8. CONCLUSIONS

In the present work, performance analysis of smoke tube boiler for waste heat recovery is carried out. The CFD simulation of the waste heat recovery boiler is done. The temperature error of analytical and CFD for flue gas is 10% and for water 5.4%. So, to minimize the error fine meshing is required at very small surfaces, which are part of a larger surface, but where they rise to form an edge of a component, this will require very small meshing elements.

REFERENCES

[1] *Shubham Agarwal , Amit Suhane, 'Study of boiler maintenance for enhanced reliability of system a review', Journal of Materials Today: Proceedings Vol.4, pp.1542-1549.*

[2] *M.C. Barma, et al., 'A review on boiler energy use, energy savings, and emissions reductions', Journal of Renewable and Sustainable Energy Reviews, Vol.79,pp. 970-983.*

[3] *Ram Thakar, et al., 'Design of heat exchanger for waste heat recovery from exhaust gas of diesel engine', Procedia Manufacturing, Vol.20,pp.372-376.*

[4] *Elliot Woolley, et al., 'Industrial waste heat recovery: A systematic approach', Journal of Sustainable Energy Technologies and Assessments Vol.29,pp.50-59.*

[5] *M.A. Gomez, et al., 'Steady CFD combustion modelling for biomass boilers: An application to the study of the exhaust gas recirculation performance',Journal of Energy Conversion and Management, Vol.179,pp. 91-103.*

[6] *Ratchaphon Suntivarakorn, et al., 'Improvement of Boiler's Efficiency Using Heat Recovery and Automatic Combustion Control System', Energy Procedia Vol.100,pp.193-197.*

[7] *C P Kothandaraman, S Subramanyan, "Heat and mass transfer data book 8th edition" ,new age international publishers.*

[8] *Standards of Tubular Exchanger Manufacturers Association, 9th edition, 2007.*

[9] *Panagiotis Drosatos, et al., 'An in-house built code incorporated into CFD model for the simulation of boiler's convection section', Journal of Fuel Proceeding Technology, Vol.202,pp. 106333.*

[10] *A. Zargoushi, et al., 'CFD modeling of industrial cold box with plate-fin heat exchanger:Focusing on phase change phenomenon',International Journal of Heat and Mass Transfer.*

[11] *Chamil Abeykoon, 'Compact heat exchanger-Design and optimization with CFD', International Journal of Heat and Mass Transfer, Vol.146,pp. 118766.*

[12] *Wei-Wei Wang, et al., 'Experimental and numerical investigations of a radial heat pipe for waste heat recovery', Journal of Applied Thermal Engineering, Vol.154,pp. 602-613.*

[13] *M. Manickam, et al., 'CFD modelling of waste heat recovery boiler', Journal of Applied Mathematical Modelling, Vol.22,pp. 823-840.*

[14] *Rupesh Suryavanshi, et al., 'A Review on Waste Heat Recovery in Industries', International Journal of Research in Advent Technology, Vol.5, No.4, April 2017.*

Chapter 4

The Applications, Methodology and Characterization of Nano Ferrite

Dhiraj Meghe[1], Nandkishor Meshram[2], Jitendra Bhaiswar[3], Samiksha Paunikar[4], Divya Lande[5], Pallavi Toney[6]

[1,3,4,5] *Department of Physics, Nagpur Institute of Technology, Nagpur*
[2] *Department of Physics, Dr. Ambedkar College, Nagpur*
[6] *Department of Physics, Saraswati Junior college, Nagpur*

ABSTRACT

In the present era many researcher are focusing on Nano ferrites due to their exponentially diverse applications in catalysts, magnetic shielding, organic transformation, magnetic recording devices, electronic devices, medical devices, transformers care, information storage, microwave absorption and many more. This chapter focused on present state of Nano ferrites with different substitution along with their synthesis methodology, characterization and application. Synthesis of Nano ferrites by co-precipitation, solid state and sol-gel method and characterization to investigate structural, electrical, and magnetic and microwave absorption is also covered in the present chapter.

Key words: Nano ferrites, Zinc-cadmium Nano ferrites, Methodology, Characterization.

1. Introduction

Nano ferrite investigations is considered to be the most important area for researchers as it has lot of technological application. Since past few decades lot of research work is carried on the synthesis of novel magnetic materials in ferrites with new characterization such as structural, electrical, magnetic and microwave absorption. Basically, ferrites are materials composed of iron oxide and bivalent elements like Zn, Ni, Mn, Cu, Mg, Cd, etc. Ferromagnetic materials have an uneven magnitude of magnetic moment and opposite direction alignment when exposed to a magnetic field [1,2]. The advantage of ferrites include high permeability, high electrical resistivity, high temperature stability, wide frequency range, high saturation magnetization, low coactivity, low eddy current loss and low cast [2,4]. The ferrites are classified as a hard ferrites and soft ferrite. The soft ferrite is the ferromagnetic materials that are not able to hold their magnetism after magnetized. These materials are easily demagnetized and magnetized with a tiny hysteresis loop. They can be created by heating and slowly cooling them. The soft ferrites has high value of permeability and susceptibility and low value of eddy current losses retentinity coercivity. They are used in electro magnets, cores of transformer etc. [2,3]. After being magnetized, the hard ferrites are unique in that they can retain magnetism. These materials have a large hysteresis loop and are difficult to magnetize and demagnetize. They are created by heating and abruptly cooling. The hard ferrites have high value of retentivity, eddy current losses, coercitivity and low value of susceptibility and permeability. They are used in permanent magnet, loud speakers etc [2]. The spinel ferrites are the combination of oxides, silicates and germinate. The chemical composition of spinel ferrites is $M^{2+}Fe_2^{3+}O_4$ where M^{2+} represent divalent metal ions such as Mg, Mn, Ni, Zn, Co, etc., Fe_2^{3+} represent trivalent metal ions and O is oxygen. With two types of interstitial gaps for the metal ions—tetrahedral (A) sides and octahedral (B) sides—the oxygen ions in the spinel structure are securely bonded in a face-centered cubic lattice (FCC). Normal and inverse spinel structures make up the grouping of spinel ferrites. Trivalent ions fully fill the octahedral (B) sides of regular spinel, while the divalent metal ion

(M^{2+}) fully occupies the tetrahedral (A) sites. The octahedral (B) side of an inverse spinel is entirely occupied by the divalent metal ion (M^{2+}), whereas the trivalent ions (fe_2^{3+}) are equally distributed between the tetrahedral (A) and octahedral (B) sites. In these materials 8A sides and 16B sites are occupied by metallic ions [4,5,6,7,8,9,10]. The spinel ferrite have high electrical resistivity, moderate coercivity, low eddy current losses, [11,12], low melting point [13], chemical stability [14] and can be easily magnetized or demagnetized. The spinel ferrites finds application in medical devices, drug delivery [2], electronic device, catalyst, transformer core, digital tape, sensor and radio frequency application [11,12,13,14,15,16].

Three series, namely the iron-spinel, chromium-spinel, and aluminum-spinel series, can be used to divide the spinel gathering (Figure 1). The four types of aluminum spinel are galaxite ($MnAl_2O_4$), hercynite ($FeAl_2O_4$), gahnite ($ZnAl_2O_4$), and spinel ($MgAl_2O_4$). Aluminum spinel is utilized in the gem business because it is translucent, stronger, and less dense than other spinel. The mineral chromium spinel is a hard, metallic black oxide. The basic member of chromium spinel series is chromite (FeCr2O4) and another member is magnesiochromite (MgCr2O4). The iron-spinel (spinel ferrite) are hard, having low coercivity and black to brownish. The iron spinel is found as Trevorite (NiFe2O4), Cuprospinel (CuFe2O4), Magnesioferrite (MgFe2O4), Jacobsite (MnFe2O4), Magnetite (Fe3O4), [2].

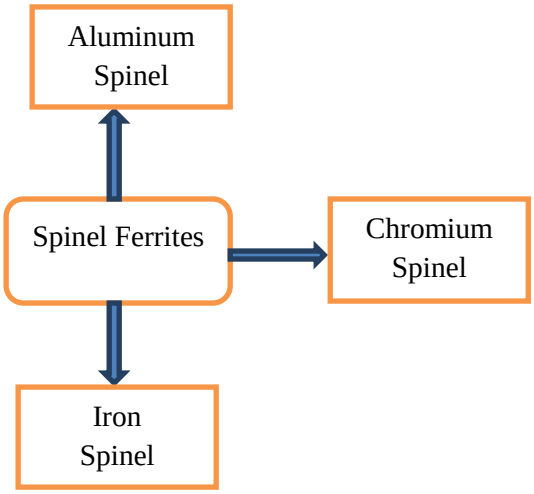

Figure 1. *Types of spinel structure*

2. SYNTHESIS OF NANO FERRITES

2.1 Sol Gel Method

The multi-step route known as "sol gel" includes chemical and physical steps related to polymerization, densification, gelation, condensation, drying, and hydrolysis. Figure 2 illustrates the ferrite manufacturing process using the sol gel method. Materials are extracted from chemical solutions by gelation in the sol gel process. There are two primary pathways: the inorganic pathway using metal salts in an aqueous solution (chloride, nitrate, oxychloride) and the metal-organic pathway using metal alkoxides in an organic solvent. Compared to metal alkoxides, the inorganic method is far less expensive and simpler to manage, but controlling the reactions is more challenging. More precise control over the phase formation, particle size homogeneity and intended stoichiometry are possible using the Sol Gel technique [17, 19]. Because it is less expensive, doesn't require specialized equipment, and can work at temperatures between 25 to 200°C—much lower than those of conventional solid-state reactions—the sol-gel technique is frequently used. Ferrites with exact morphologies, such as fibers, microspheres, and flower-like structures with a restricted size distribution, can be created using the sol-gel technique. The sol gel method has some drawbacks as well, including the need for expensive raw materials compared to high carbon content in the products, mineral-based metal ion sources, multiple steps, the need for close process monitoring, a lengthy processing time, and challenges with phase separation [18].

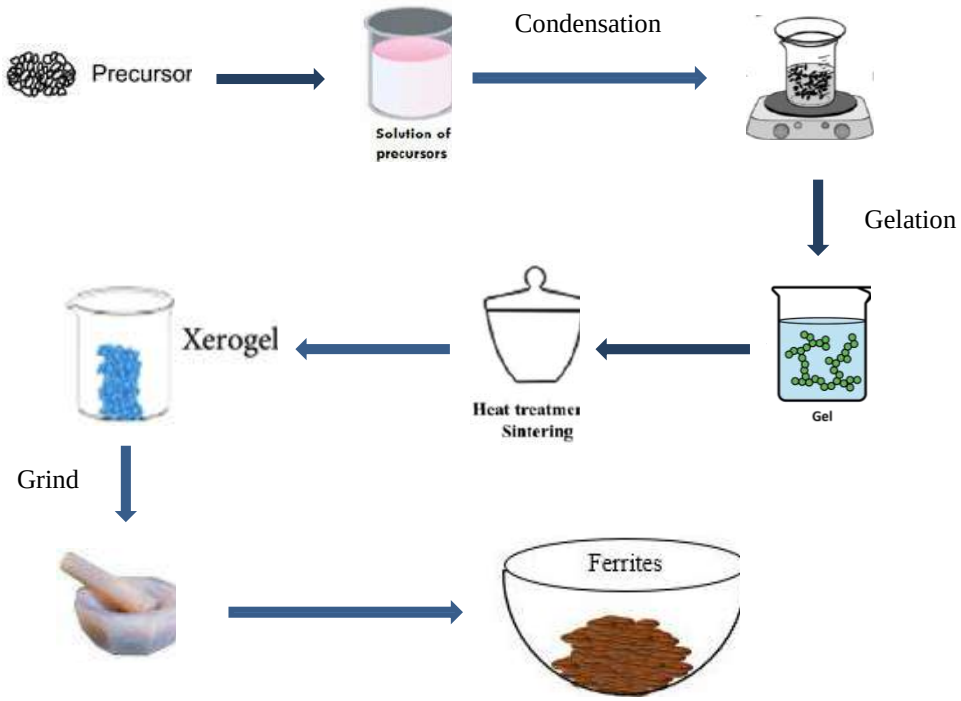

***Figure 2**. Synthesis process by Sol-Gel Method*

2.2 Solid State Method

A wide range of materials, such as nitrides, sulfides, aluminosilicates and mixed metal oxides, can be manufactured using the traditional ceramic process. This synthesis method requires several steps, starting with the homogenization of two or more solid compounds, which is followed by grinding in a wet medium to control particle size and create a homogenous blend, compaction, and heating the mixture at a high temperature, as illustrated in Figure 3 [20,21].

Polycrystalline solids are frequently created from a mixture of solid reactants via solid-state processes. High temperatures are needed to start a reaction because mixtures of solids do not react at room temperature for very long (chemical breakdown of reactants). Surface area, reactivity, free energy change, and other chemical characteristics and morphological of the reactants all have an impact on these processes [22]. In addition to producing complicated oxides, these processes are used to make advanced materials such as piezoelectrics. To create a new solid alignment with gas development, physical mixing of simple oxides, nitrates, hydroxide, carbonate, alkoxides, oxalates, sulphate, or other metal salts is followed by high temperature treatment, typically between 1000°C and 1500°C [23]. Large-scale production of ferrite materials with a high yield and minimal pollution is possible through solid-state processes [24].

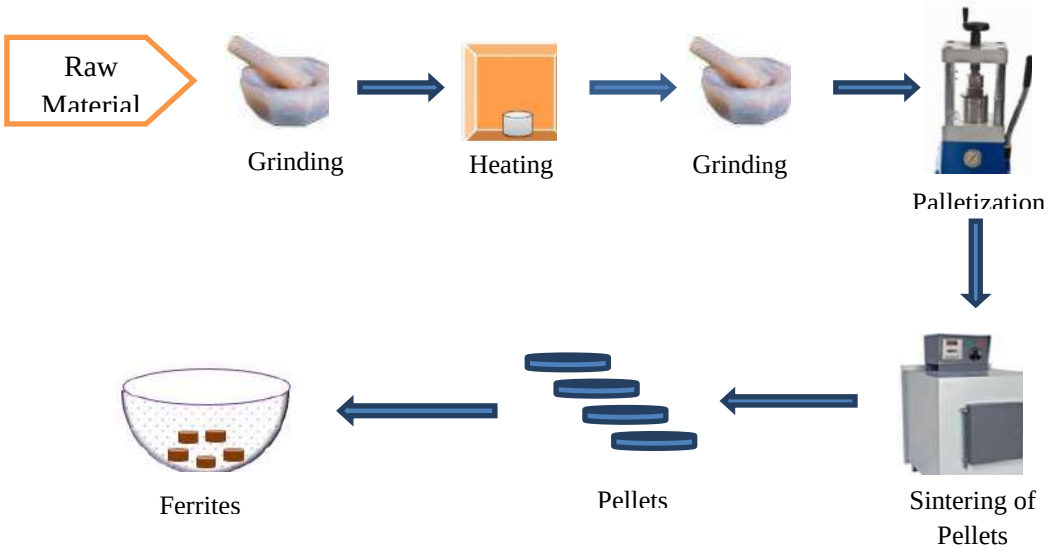

***Figure 3**. Synthesis process by solid state Method*

2.3 co-precipitation method

The easiest and most practical way to create magnetic particles is by chemical co-precipitation. Using this method, two or more cations precipitate to produce a uniform composition [25]. Four steps make up this method: nucleation, growth, coarsening, and agglomeration all occur simultaneously [26]. The co-precipitation method involves introducing a mixture solution containing cation chloride (Fe, Sr, etc.) dropwise into a solution of $NaOH/Na_2CO_3$. This process produces precipitation. To create HFs, cations with carbonate or nitrate can be substituted for chloride cations. In contrast, hydrochloric acid transforms cations of carbonate, like $SrCO_3$, into cations of chloride in the latter scenario. After filtering and ethyl alcohol washing the precipitates until no NaCl is visible, the pH is maintained below 8. As illustrated in Figure 4, the cleaned precipitates are dried and calcined for three hours at 950 °C.

Some benefits of this approach include its simplicity, ease of controlling particle size, uniformity of small-sized nanomaterials, energy-efficient bulk production of magnetic nanoparticles, etc. The method's drawbacks include trace impurity, time consumption, and nanoparticle instability [26].

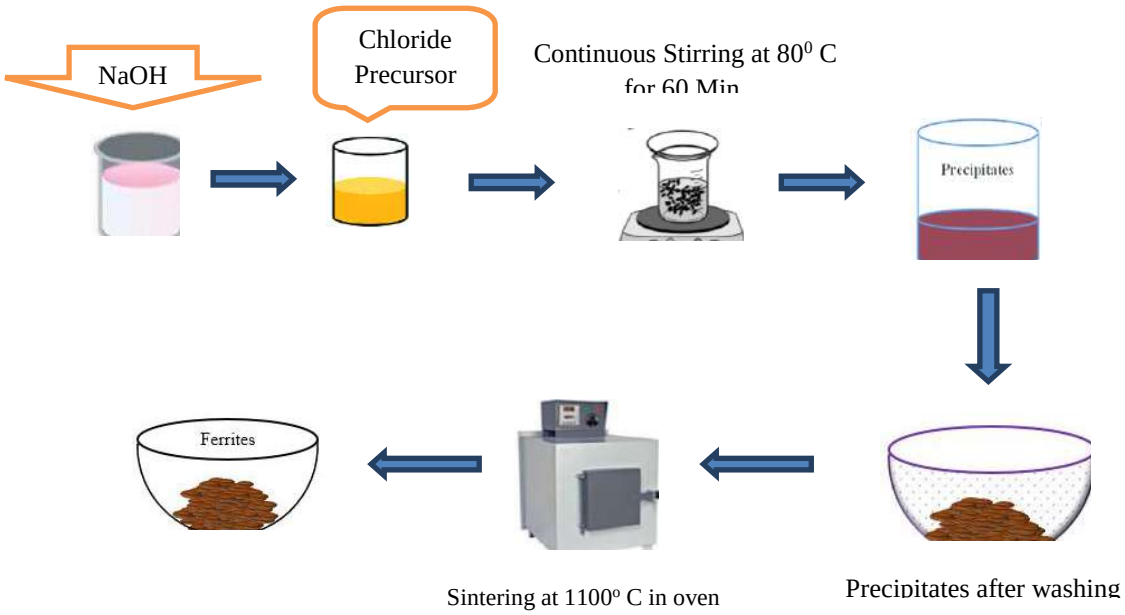

***Figure 4**. Synthesis process by co-precipitation Method*

Chapter 4

3. CHARACTERIZATION NANO FERRITES

To look into structural, electrical, magnetic, and microwave absorption, characterization is done.

3.1 Structural Property

According to the XRD principle, constructive interference happens for a fixed set of incidence angle (θ) and interplanar spacing (d) for a given wavelength (λ). Bragg's has provided a mathematical equation that relates the incident X-ray wave length, the layer's distance, and the angle of diffraction [27].

$$2\,d\sin\theta = n\,\lambda \qquad (1)$$

where n = (1, 2, 3, 4, …etc.)

The crystallite size can be calculated by Debye-Scherrer equation as follows [28].

$$D = \frac{0.9\,\lambda}{\beta\cos\theta}$$

Where, D = Size of crystallite (in nm), β = full width at half maximum of the peak (in radians), λ = X ray wavelength (λ = 1.5406 Å), θ = Bragg's angle (in radians),

The lattice dimension (a) is calculated by following formula [29]

$$d = \frac{a}{\sqrt{h^2+k^2+l^2}}$$

Where, d = interplanar spacing and h, k and l are the miller indices.

The true density (X-ray density) is calculated by the relation which is given bellow [37]

$$D_x = \frac{Z\,M}{N_a\,a^3}$$

Where, M = Molecular weight of the sample, a=lattice constant, N=Avagadro number.

Now, the porosity (p) of the ferrite is can be calculated as follows [29]

$$p = 1 - \frac{D}{D_x}$$

Where, D = apparent density of the prepared sample

The real crystal structure, crystallite size and strain, long range order, porosity, phase identification, unit cell volume, etc. of ferrites are all ascertained by X-ray diffraction (XRD) [30, 31].

3.2 Scanning Electron Microscopy

SEM is used to examine the morphological properties of the resultant nano-ferrite. High-energy electrons are scanned across a ferrite surface to produce images [32]. These concentrated electrons interact with the different atoms in the ferrite to produce heat, visible light, secondary electrons, diffracted backscattered electrons, a characteristic X-ray, and other signals when they collide with the ferrite surface. It alludes to the investigation of ferrites' size, shape, and structure.

3.3 FTIR Spectroscopy

It is the technique that is most frequently used to identify the functional groups in Cd ferrites that are produced. In order to do this, the sample is exposed to an infrared radiation between 400 and 4000 cm^{-1}, and the molecular structure is ascertained by measuring the absorbance of these radiations by ferrite. Rather than often producing electrical excitation, infrared radiation produces vibration excitation, which causes the bond connecting atoms or groups of atoms to vibrate more quickly. Plotting the substance's absorbance of infrared light in contradiction of its wavelength, the FT-IR

spectrometer creates an IR spectrum [33]. Table 4 reports some of the ferrites tetrahedral bond and octahedral bond from FTIR Analysis

3.4 Vibrating sample magnetometer

Utilizing Faraday's principle of induction, a vibrating sample magnetometer (VSM) examines the magnetic properties of magnetic materials [34, 35]. In vector signal modulation (VSM), a fluctuating magnetic field generates an electric field, which provides information about the fluctuating magnetic field. Saturation magnetization, Hysteresis loop, remanence, coercivity, and magnetic moment can all be analyzed using VSM data [34, 35, 36]. Table 5 reports some of the ferrites magnetic properties from VSM Analysis

4. Conclusion

Ferrites' basic characteristics, research trend, properties, and classification were all covered. For the preparation of Nano ferrites, the most popular techniques— chemical co-precipitation, sol gel, and solid state methods—were contrasted. The XRD is used to calculate the structure, crystallite size, and properties of ferrites. The SEM micrographs demonstrated that substitutions and their doping percentage level have a significant impact on the microstructure development, morphology, and grain size. The formation of the nano ferrites with different dopant elements was confirmed by the FTIR study. The position of both bonds changed from their initial positions with distinct substitutions, can be calculated by the FTIR analysis. The impact of substitutions, grain size, doping percentage level, and temperature on the magnetic properties of ferrites was revealed by an insight into a vibrating sample magnetometer.

References

[1] *Adam JD, Davis LE, Dionne GF, et al. (2002) Ferrite devices and materials. IEEE T Microw Theory 50: 721–737.*

[2] *Ajitanshu Vedrtnam, Kishor Kalauni, Sunil Dubey and Aman Kumar (2020) Material Science: A comprehensive study on structure, properties, synthesis and characterization of ferrites. AIMS Material Science 7: 800-835*

[3] *Pullar RC (2012) Hexagonal ferrites: A review of the synthesis, properties and applications of hexaferrite ceramics. Prog Mater Sci 57: 1191–1334.*

[4] *Santosh Bhukal, S. Bansal, Sonal Singhal, Journal of Molecular Structure 1059 (2014) 150–158*

[5] *Arun Vijay Bagade, Pratik Arvind Nagwade, Arvind Vinayak Nagawade, Shankar Ramchandra Thopate And Sangita Nanasaheb Pund, A Review on Synthesis, Characterization and Applications of Cadmium Ferrite and its Doped Variants orient. J. Chem., Vol 38(1), 01-15 (2022)*

[6] *M.A. Yousuf, S. Jabeen, M.N. Shahi, M.A. Khan, I. Shakir, M.F. Warsi, Results Phys. 16 (2020) 102973.*

[7] *Sickafus, K. E.; Wills, J. M.; Grimes, N. W. J. Am. Ceram. Soc., **1999**, 82, 3279–3292.*

[8] *Harpreet Kaur, Amrik Singh, Vijay Kumar, Dharamvir Singh Ahlawat Structural, thermal and magnetic investigations of cobalt ferrite doped with Zn^{2+} and Cd^{2+} synthesized by auto combustion method Journal of Magnetism and Magnetic Materials 474 (2019) 505–511*

[9] *W. Zhongli, L. Xiaojuan, L. Minfeng, C. Ping, L. Yao, M. Jian, J. Phys. Chem. 112 B (2008) 11292.*

[10] *V.S. Kumbhar, A.D. Jagadale, N.M. Shinde, C.D. Lokhande, J. Appl. Surf. Sci 259 (2012) 39.*

[11] *Paramesh D, Kumar KV, Reddy PV (2016) Influence of nickel addition on structural andmagnetic properties of aluminium substituted Ni–Zn ferrite nanoparticles. Process Appl Ceram 10: 161–167.*

[12] *Singh S, Ralhan NK, Kotnala RK, et al. (2012) Nanosize dependent electrical and magneticproperties of NiFe2O4 ferrite. IJPAP 50: 739–743.*

[13] *Nejati K, Zabihi R (2012) Preparation and magnetic properties of nano size nickel ferrite particles using hydrothermal method. Chem Cent J 6: 23.*

[14] *Melagiriyappa E, Jayanna HS (2009) Structural and magnetic susceptibility studies of samarium substituted magnesium-zinc ferrites. J Alloy Compd 482: 147–150.*

[15] *Lazarević ZŽ, Jovalekić Č, Sekulić D, et al. (2012) Characterization of nanostructured spinel NiFe2O4 obtained by soft mechanochemical synthesis. Sci Sinter 44: 331–339.*

[16] *Gözüak F, Köseoğlu Y, Baykal A, et al. (2009) Synthesis and characterization of CoxZn1−xFe2O4 magnetic nanoparticles via a PEG-assisted route. J Magn Magn Mater 321: 2170–2177.*

[17] *Peterson DS (2013) Sol-gel technique, In: Li D, Encyclopedia of Microfluidics and Nanofluidics, New York: Springer Science + Business Media, 1–7.*

[18] *Muresan LM (2015) Corrosion protective coatings for Ti and Ti alloys used for biomedical implants, In: Tiwari A, Rawlins J, Hihara LH, Intelligent Coatings for Corrosion Control, Boston: Butterworth-Heinemann, 585–602.*

[19] *Xu P (2001) Polymer-ceramic nanocomposites: ceramic phases, In: Buschow KHJ, Cahn RW, Flemings MC, et al., Encyclopedia of Materials: Science and Technology, Oxford: Elsevier, 7565–7570.*

[20] *Šepelák V, Bergmann I, Feldhoff A, et al. (2007) Nanocrystalline nickel ferrite, NiFe2O4: Mechanosynthesis, nonequilibrium cation distribution, canted spin arrangement, and magnetic behaviour. J Phys Chem C 111: 5026–5033.*

[21] *Rao CNR, Biswas K (2015) Ceramic methods, Essentials of Inorganic Materials Synthesis, John Wiley & Sons, 17–21.*

[22] *Cho, S. J.; Uddin, M. J.; Alaboina, P. "Emerging Nanotechnologies in Rechargeable Energy Storage Systems", **2017**, 83-129, doi:10.1016/ b978-0-323-42977-1.00003-0.*

[23] *Buekenhoudt, A.; Kovalevsky, A.; Luyten, Ir J.; Snijkers, F. Basic Aspects in Inorganic Membrane Preparation in "Comprehensive Membrane Science and Engineering"., **2010**, 1, 217-252.*

[24] *Dao-hua, L.; Shao-fen, H.; Jie, C.; Chengyan, J.; Cheng Y. IOP Conf. Ser.: Mater. Sci. Eng., **2017**, 242, 012023.*

[25] *Liu S, Ma C, Ma MG, et al. (2019) Magnetic nanocomposite adsorbents, In: Kyzas GZ, Mitropoulos AC, Composite Nanoadsorbents, Elsevier, 295–316.*

[26] *Rane AV, Kanny K, Abitha VK, et al. (2018) Methods for synthesis of nanoparticles and sabrication of nanocomposites, In: Bhagyaraj MS, Oluwafemi OS, Kalarikkal N, et al., Synthesis of Inorganic Nanomaterials, Woodhead Publishing, 121–139.*

[27] *Chatterjee AK (2001) X-ray diffraction, In: Ramachandran VS, Beaudoin JJ, Handbook of Analytical Techniques in Concrete Science and Technology: Principles, Techniques and Applications, Norwich, New York: William Andrew Publishing, 275–332.*

[28] *Kumar, C. G.; Pombala, S.; Poornachandra, Y.; Agarwal, S. V. Nanobiomaterials in Antimicrobial Therapy, Applications of Nanobiomaterials., **2016**, 6, 103-152.*

[29] *Nikumbh, A. K.; Nagawade, A. V.; Gugale, G. S.; Chaskar, M. G.; Bakare; P. P. J. Mater. Sci., **2002**, 3(7), 637–647.*

[30] *Moscoso-Londoño O, Tancredi PABLO, Muraca D, et al. (2017) Different approaches to analyze the dipolar interaction effects on diluted and concentrated granular superparamagnetic systems. J Magn Magn Mater 428: 105–118.*

[31] *Liu Q, Liu Y, Wu C (2017) Investigation on Zn–Sn co-substituted M-type hexaferrite for microwave applications. J Magn Magn Mater 444: 421–425.*

[32] *McMullan, D. Scanning electron microscopy 1928-1965, Scanning., 1995, 17, 175–185.*

[33] *Silverstein, R.; Webster, F.; Kiemle, D., Spectrometric Identification of Organic Compounds, John Wiley and Sons Inc., New York., 2006.*

[34] *Manju BG, Raji P (2018) Synthesis and magnetic properties of nano-sized Cu0.5Ni0.5Fe2O4 via citrate and aloe vera: A comparative study. Ceram Int 44: 7329–7333.*

[35] *Dairy ARA, Al-Hmoud LA, Khatatbeh HA (2019) Magnetic and structural properties of barium hexaferrite nanoparticles doped with titanium. Symmetry 11: 732.*

[36] *Nikumbh, A. K.; Nagawade, A. V.; Gugale, G. S.; Chaskar, M. G.; Bakare; P. P. J. Mater. Sci., **2002**, 3(7), 637–647.*

[37] *Salma Ikram, Jolly Jacob, M.I. Arshad, K. Mahmood, A. Ali, N. Sabir, N. Amin, S. Hussain, Tailoring the structural, magnetic and dielectric properties of Ni-Zn- CdFe2O4 spinel ferrites by the substitution of lanthanum ions Ceramics International 45 (2019) 3563–3569*

Chapter 5

Heuristic Based Clustering For Macula Segmentation and Fovea Localization

Dr. Malpe Kalpana Devidas[1], Mr. Shewale Shubham Shivaji[2]

[1]Assistant Professor, [2]M.Tech Student
Department of Computer Science and Engineering, Gurunanak Institute of Engineering and Technology, Nagpur, Maharashtra, India.

shubh.shewale18@gmail.com

ABSTRACT

Macula is a significant structural pattern responsible for high resolution vision. Existing approaches towards extraction of macula and fovea mostly involve segmentation of optic disc and identifying macula with optic disc as reference. This is a computationally complex and error prone task. This work attempts to utilize data mining techniques for this purpose. Since macula lacks well defined border definition and no expert opinion is provided in this regard, supervised classification techniques cannot be adopted. Unsupervised clustering technique is sought for this purpose. This chapter introduces an unsupervised clustering algorithm for segmentation of macula. The algorithm targets at incorporating a heuristic based on measures indicating the statistical distribution of data for selecting the initial cluster centers that play a significant role in performance of the clustering algorithms. Initially, the clustering algorithm is explained. Then, the significance of extraction of macula region is quoted which is followed by the proposed methodology to serve the purpose. Then, the results are presented with respect to the literature. The following section deals with the heuristic based clustering algorithm.

Keywords: - *Macula, Segmentation, Data Mining Techniques, Clustering, Unsupervised Clustering, fovea, heuristic based Clustering.*

INTRODUCTION

5.1 HEURISTIC BASED CLUSTERING ALGORITHM

This section discusses the proposed clustering algorithm. On analysing clustering algorithms, it is observed that the initial cluster centre selection influences the performance of clustering process greatly (Hartigan 1975). Commonly and extensively used heuristics for this purpose include random selection of all the cluster centres or random selection of one centre followed by choosing the other centres through a heuristic or choosing every centre through heuristics. To begin with, datasets with less number of instances and that belong to two class category were chosen from public repositories for investigation. Then, all combinations of cluster centres were worked out to analyse the performance of the partitioning. It was interesting to note that a very few combination of initial cluster centres yielded very high accuracy in partitioning. It was higher than that obtained from the previous commonly adopted heuristics. Hence, attempts are made to find the cluster centre combination through some formulated heuristic. At first, trials are made to find one of the two cluster centres. After obtaining one cluster centre, the logic for identifying the other cluster center is devised. On analysing, the metrics that defined the statistical distribution viz., minimum, median,

mean, maximum and skew appear appealing for the purpose of partitioning. The following paragraphs explain the proposed heuristic.

The proposed clustering algorithm utilises the metrics that represent the statistical distribution of data for initial selection of cluster centres. It is well suited for the cases where there exists two groups and the data attributes are continuous. Hence, the algorithm can be applied to image segmentation where the anatomical structure is one group and the background forms the other group. Additionally, the features representing each pixel of the image belong to the category of continuous attributes. The proposed algorithm attempts to choose two cluster centres and the outcome results in two groups such that the intra cluster similarity is less and the inter cluster distance is high. The heuristic first chooses the first centre followed by the selection of the second centre. The steps followed in the algorithm to choose the first cluster centre is shown in Figure 5.1.

Step 1: Compute the skew of entire data by summing the skew of every dimension. Skew of every dimension A_j is calculated as follows:

$$skew(A_j) = \frac{\frac{1}{n}\sum_{i=1}^{n}(x_i - \mu)^3}{(\sqrt{\frac{1}{n}\sum_{i=1}^{n}(x_i - \mu)^2})^3}$$

Where μ is the mean of the data and n is the number of samples

$$entireskew = \sum_{j=1}^{m} skew(A_j)$$

Where m is the number of dimensions

Step 2: Find the covariance of all attributes with respect to the first attribute

$$cov(A_1, A_j) = \frac{1}{N-1}\sum_{i=1}^{N}(A_{1_i} - \mu_{A_1})(A_{j_i} - \mu_{A_j})$$

Step 3: Compute a minimum_feature_vector such that
For each attribute, find the
min_value if it is has positive or zero covariance
max_value if it has negative covariance.

Step 4: Find euclidean distance between the formed feature vector and every instance of the dataset and arrange the data in ascending order with respect to its distance from the minimum feature vector.

Step 5: The instances having minimum, median and maximum distance are chosen as candidates for the first centre (FCC).

Step 6: For each instance I in FCC, remove the instance and find skewness of the remaining instances remskew(I)

Step 7: Find its difference diff(I)=entireskew-remskew(I).

Step 8: The first centre (FC) is the instance I which has maximum diff(i) and the corresponding remskew be skewfc.
Having chosen the centre for the first cluster, it should be either the minimum, median or maximum instance

Figure 5.1 Procedure for selection of first cluster centre

The proposed algorithm initially computes the skew of the entire data. Then, it calculates the covariance of all attributes of the data with the first attribute. Then, a minimum feature vector is formulated based on the covariance of each attribute with the first attribute. It is formed such that if the attribute has a positive covariance, then the minimum value of the attribute is taken; else the maximum value of the attribute is chosen. Then, the distance of every data instance is computed with respect to the minimum feature vector formulated. The data instances are then sorted in ascending order based on the distance obtained from the previous calculation. The instances that are at minimum, median and maximum distance from the minimum feature vector are shortlisted as candidates for first cluster centre and investigated further. Again, skew of the data is calculated after removing the minimum , median and maximum instances with replacement .The difference between the skew of the data after removing the instances and skew of the entire data is computed. The instances, whose removal led to the minimum difference, is chosen as the first cluster centre (FC). Having chosen the first cluster centre, it should either be the minimum, median or maximum instances. Now, the other centre is chosen based on the first centre as given in Figure 5.2.

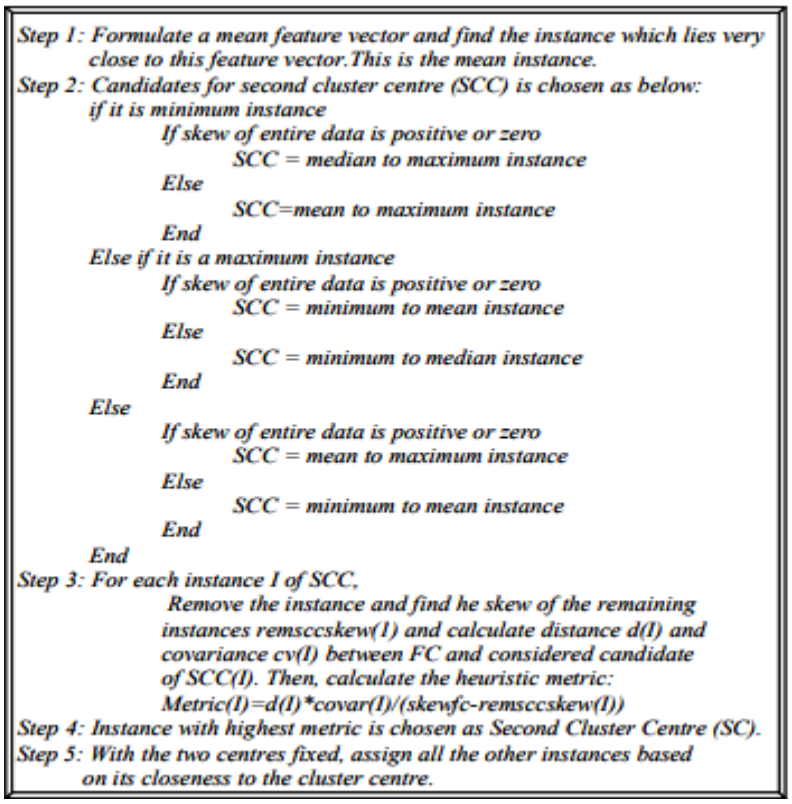

Figure 5.2 Procedure for selection of second cluster centre

The second cluster centre is chosen based on the following notion. Having chosen the FC, it should be either the minimum, maximum or median instance. Then, a mean instance is formulated for the subsequent investigations. The mean instance will lie between the median and maximum instance, if the data is positively skewed. It will be located between the minimum and median instance if the data is negatively skewed. So, if FC is a minimum or maximum instance, the other centre that produces best grouping is expected to be in another subset, where the subsets are separated by median or by mean instance. The superset between the two subsets is always chosen as the candidates for second cluster centre (SCC).

Based on this concept, the candidates for the second cluster centre are chosen as follows: If FC is a minimum instance and entire skew is positive, the second cluster centre (SC) that yields best partitioning is expected to lie between the median instance and the maximum instance (superset between subsets formed from (i) median instance and maximum instance and (ii) mean instance and maximum instance). Otherwise, if FC is minimum and skew is negative, then SC is expected to lie between the mean and the maximum instance. Similarly, if FC is a maximum instance, then the candidates for SC will be located between minimum and mean instance if the data is positively skewed while it is expected to lie between minimum and median instance if the data is negatively skewed. If FC is a median instance in a positively skewed data, then the candidates for SC are expected to lie between mean and maximum instance. If FC is a median instance in the negatively skewed data, then, the instances from minimum to mean are included in SCC.

The proposed clustering is very useful in grouping continuous data as skew is meaningful for continuous data only. This algorithm can therefore be utilised for the task of image segmentation, where a particular region have to be segmented and the remaining areas are considered as the background. This algorithm is adopted to segment the macula of the retinal fundus images. The proposed methodology incorporating the proposed clustering algorithm for segmentation of macula is presented in the following section.

5.2 MACULA SEGMENTATION AND FOVEA LOCALISATION

Chapter 5

This section discusses the proposed methodology to segment macula, a structural pattern. To begin with, the importance of extracting macula is highlighted. Followed by this, the proposed methodology is detailed. The subsequent sub-section deals with the significance of macula segmentation.

5.2.1 Significance of macula segmentation

The macula is a round area in the central region of the retina, which measures about 3 to 4 mm in diameter (Helga Kolb 2011). It provides high resolution vision and is responsible for central vision. There is a small depression in the centre of the macula measuring around 1 mm in diameter and appears as a round dark area called the fovea (Patton et al 2006). The macula exhibits non-specific structure and varies greatly across individuals due to variations in the levels of pigmentation associated with factors such as ethnicity, age, diet and disease conditions. Anatomically, the fovea centre is located at 2.5 optic disc diameter (DD) from the optic disc (OD) centre. The radius of the macula region is approximately equal to 1 DD (Schwiegerling 2004). This region is devoid of vessels. A sample fundus image showing an annotated macula is illustrated in Figure 5.3.

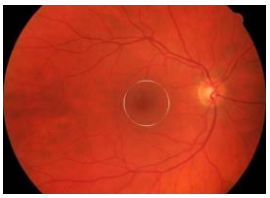

Figure 5.3: Sample fundus image showing annotated macula

5.2.2 Proposed methodology for macula segmentation and fovea localisation

The proposed framework segments the macula from the retinal fundus image through three phase's viz. image pre-processing, data mining and image post-processing phases. The proposed framework is portrayed in Figure 5.4

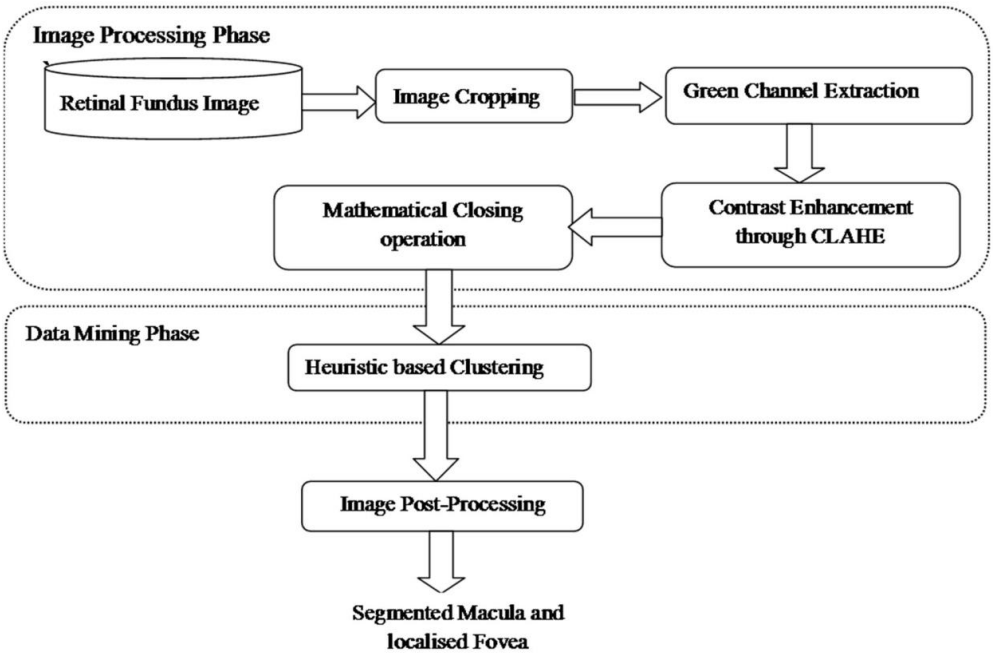

Figure 5.4 Proposed framework for macula segmentation

Chapter 5

The proposed methodology begins with the image pre-processing phase, during which the image is cropped to the desired extent and the green channel image is extracted and contrast enhanced through CLAHE. The intensities of this image are given as input to the proposed clustering algorithm which results in a binary map with many candidate components for macula. Then, image post-processing is performed to eliminate the unwanted components and choose the macula component. The centre of the macula component is the fovea.

To start with, the proposed framework employs image pre- processing techniques. Initially, the image is cropped to delineate the field of view. Then, the upper quarter and lower quarter of the image is eliminated in the view that the macula is mostly found only in the central region of the fundus image, along the line which separates the inferior and superior part of the fundus. The elimination of lower and upper quarters reduces the computational complexity in the forthcoming steps. After cropping the image, the green channel image of the RGB color model is extracted. As this channel exhibits the contrast very well, macula is clearly visible. Then, the green channel image is contrast enhanced through CLAHE procedure (Piezer et al 1987) explained in the previous chapter, to exhibit the macula more prominently.

Sample illustration of the outcomes of the various processes adopted during image pre-processing phase is depicted in Figure 5.5.

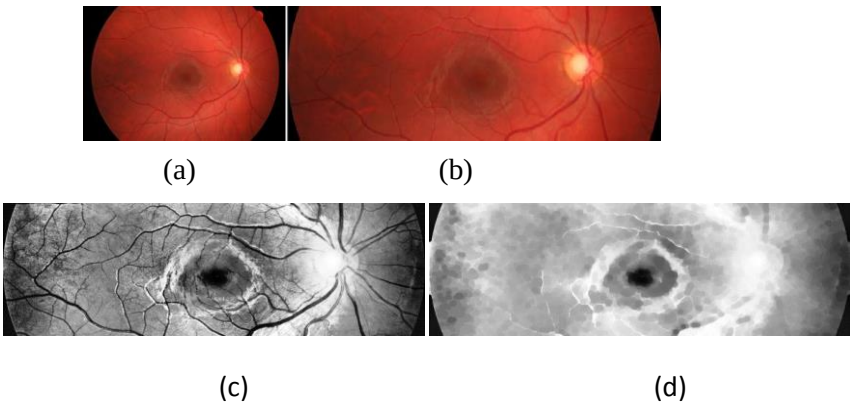

Figure 5.5 Sample images of outcomes of image pre-processing phase in macula segmentation (a) RGB, (b) cropped RGB, (c) contrast enhanced Green channel, (d) contrast enhanced Green channel after performing closing operation

The intensities of the processed Green channel image are given as input to the data mining phase. The data mining phase involves clustering of the input data into two groups namely background and candidate components for macula. The proposed heuristic based clustering algorithm is adopted for this purpose. The outcome of clustering algorithm is a binary map with a few components. This binary image is then post-processed to find the macula.

The post-processing phase initially eliminates the components whose eccentricity is higher than 0.95. Then, the extreme components, at places out of the field of view, which could not be eliminated during cropping, also appear dark and are exposed as candidates for macula. These regions are eliminated.

Out of the remaining components, each component is superimposed on the green channel image and the minimum intensity of each part is found. The component that corresponds to the minimum of the minimum intensity is chosen as the macula. The holes, if present in the identified component are filled and the component is concluded as the macula. The outcome of the data mining phase, image post-processing phase, and the RGB image showing the detected macula boundary, detected fovea centre and the annotated fovea centre are provided in Figure 5.6.

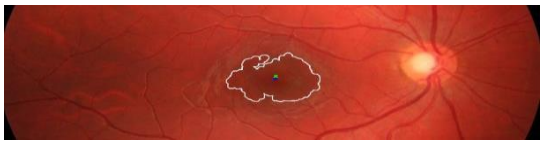

(c)

Figure 5.6 Output of data mining and image post-processing phase in macula segmentation and fovea localization (a) Data mining phase (b) Image post-processing phase (c) RGB image showing detected macula boundary, detected (+ in blue color) and marked (in green color) fovea centre*

The performance of the proposed methodology is evaluated on various benchmark datasets. The performance on segmentation of macula is exhibited in the following section.

5.3 Performance of proposed methodology in macula segmentation and fovea centre identification

The proposed methodology is evaluated using HRF (Budai et al 2011), DRIVE (Niemeijer et al 2004; Staal et al 2004), DIARETDB0 (Kauppi T et al), DIARETDB1 (Kauppi et al 2007), HEI-MED (Giancardo et al 2012), STARE (Hoover et al 2000) and MESSIDOR (Decenciere et al 2014) datasets. With regard to the MESSIDOR dataset, annotations of fovea centres created and published by the University of Huelva for 1136 images are used for performance evaluation. In contrast, since there are no publicly available annotations offered for the HRF, DRIVE, DIARETDB0, DIARETDB1, HEI- MED, STARE and remaining 64 images of MESSIDOR dataset, fovea centres were marked by experts to make performance evaluation feasible in these datasets.

This sub-section presents the performance of the proposed methodology in identifying the macula and hence the fovea centre. The proposed methodology is also implemented using K-Means clustering algorithm (MacQueen 1967; Lloyd 1982; Forgy 1965; Hartigan 1975) and the performance of K-Means and proposed clustering algorithm is exhibited revealing the better performance of the proposed clustering in this regard. Table 5.1 presents the performance of the proposed methodology in terms of number of images with correctly identified fovea location with respect to the criterion specified in the previous sub-section.

Table 5.1 Performance of the proposed methodology in macula and fovea detection

Dataset	Clustering	Excellent	Good	Fair	Poor	Excellent-Fair
HRF	K-Means	9	19	15	2	43
	Proposed	22	19	4	0	45
DRIVE	K-Means	24	7	1	3	32
	Proposed	23	12	0	0	35
DIARETDB0	K-Means	65	39	18	8	122
	Proposed	72	38	16	4	126
DIARETDB1	K-Means	21	26	31	11	78
	Proposed	46	33	8	2	87
HEI-MED	K-Means	43	55	62	9	160
	Proposed	47	55	65	2	167
STARE	K-Means	6	3	5	6	14
	Proposed	12	2	4	2	18
MESSIDOR	K-Means	996	91	75	38	1162
	Proposed	1020	109	63	8	1192

Chapter 5

On examination of the results of the proposed methodology in segmenting macula, the results justify the better performance of the proposed clustering algorithm in comparison with the K-Means clustering procedure. On computation of accuracy, it is found that the fovea centre is correctly located (satisfying the IR criterion) in 100% of HRF, 100% of DRIVE, 96.92% of DIARETDB0, 97.75% of DIARETDB1, 98.82% of HEI-MED, 90% of STARE and 99.33% of MESSIDOR images. Overall, in 98.93% of images, the fovea centre is identified within the one time OD radius from the real fovea centre. Figure 7.7 graphically represents the improved performance of the proposed clustering with regard to K-Means clustering.

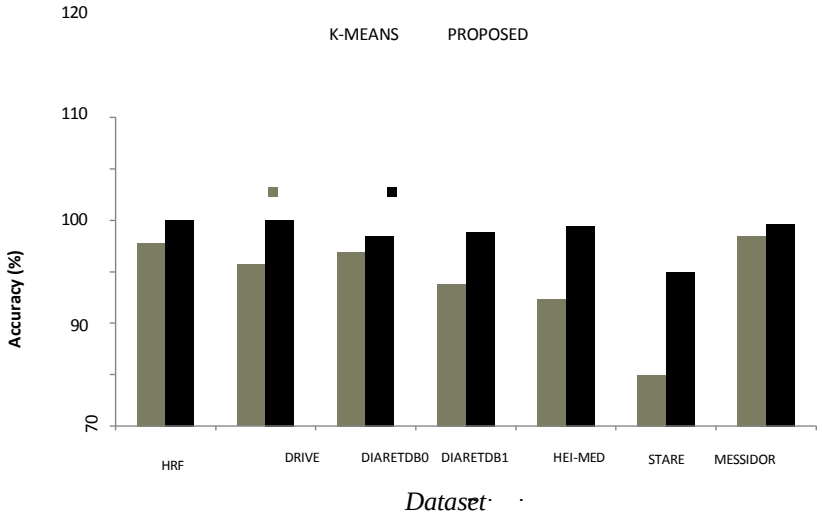

Figure 5.7 Performance comparison of proposed clustering algorithm with K-Means algorithm for macula segmentation and fovea detection

On further investigation of the results owing to the quality and the health status of the images, the following results are reported. With regard to the quality categories viz. Good, Average and Poor, the performance of the proposed methodology is exhibited in terms of satisfying Excellent (<0.25R), Good (>0.25 and <0.5R), Fair (>0.5R and <1R) and Poor (>1R) criteria. The cumulative result projecting correct fovea locations in the span Excellent to fair with respect to various quality categories is also presented in Table 5.2. The results are projected for the entire collection of 1688 images from all the datasets.

Table - Performance of the proposed methodology in macula and fovea detection owing to quality categories.

Quality Category	Excellent	Good	Fair	Poor	Excellent-Fair
Good	1007/1293	186/1293	96/1293	4/1293	1289/1293
Average	218/356	74/356	56/356	8/356	348/356
Poor	17/39	8/39	8/39	6/39	33/39

The results show the number of images in which the fovea centre is correctly located to the number of images in a particular quality category. In terms of accuracy, the results of correct prediction of the fovea centre are reported as follows: 77.88% of Good quality images satisfies the 0.25R Criterion, remaining 14.39% of Good quality images satisfies the 0.5R Criterion and left out 7.43% satisfies the 1R criterion while in 0.31% of good quality images, the detected fovea do not lie within 1R distance from the real fovea centre. This shows that in 99.69% of good quality images, the detected fovea centre lies within the IR distance of the real fovea centre. Similarly, in average quality images, 61.24%, 20.79% and 15.73% of images satisfies the 'Excellent', 'Good' and 'Fair' criteria respectively while

in 2.25% of images, the correct fovea location is not identified. Thus, in the case of average quality images, 97.75% of images have their detected fovea centres at less than the value of OD radius from the fovea centres marked by the experts. On examination of the results with respect to poor quality images, it is found that 43.59%, 20.52% and 20.52% of images satisfies 'Excellent', 'Good' and 'Fair' criteria while in 15.39% of images, the fovea centre is at a distance greater than the OD radius from the real fovea centre. This shows that in 84.62% of poor quality images, the fovea centre lies within the distance of OD radius from the annotated fovea centre.
Subsequently, analysis is performed with respect to health status of the images. Table 5.3 presents the related results.

Table- Performance of the proposed method in macula and fovea detection owing to health of the images

Health Category	**Excellent**	**Good**	**Fair**	**Poor**	**Excellent-Fair**
Healthy	551/727	103/727	67/727	6/727	721/727
Diseased	691/961	165/961	93/961	12/961	949/961

The results recorded in Table 7.3 presents the number of images in which the fovea centre is correctly located to the number of images in healthy and diseased images respectively. In terms of accuracy, the results of correct prediction of the fovea centre is reported as follows: 75.79% of healthy images satisfies the 'Excellent' criterion, remaining 14.17% of healthy images satisfies the 'Good' criterion and left out 9.22% satisfies the 1R criterion while in 0.82% of healthy images, the detected fovea do not lie within 1R distance from the real fovea centre. This shows that in 99.18% of healthy images, the detected fovea centre lies within the 1R distance of the real fovea centre. Similarly, in diseased images, 71.90%, 17.17% and 9.68% of images satisfies the 'Excellent', 'Good' and 'Fair' criteria respectively while in 1.25% of images, the correct fovea location cannot be found. Thus, in the case of diseased images, 98.75% of images have their detected fovea centres less than the OD radius from the fovea centres marked by the experts.

The results justify the utilisation of the proposed methodology in automated retinal image system. The following sub-section presents a comparison of the performance of the proposed methodology with regard to the earlier works in macula segmentation and fovea localisation.